



Aus der Klinik für Kinderkardiologie und angeborene Herzfehler

DISSERTATION

**EVALUATION OF MYOCARDIAL FUNCTION IN
PATIENTS WITH HYPERTROPHIC OBSTRUCTIVE
CARDIOMYOPATHY BY TISSUE DOPPLER
TECHNIQUE**

zur Erlangung des akademischen Grades
Doktor medicinae (Dr. med)

vorgelegt der Medizinischen Fakultät der Charité –
Universitätsmedizin Berlin

von

Ragiab Telagh

aus: Tripolis, Libyen

Gutachter: 1. Priv.-Doz. Dr. med. H. Abdul-Khaliq
2. Prof. Dr. med. W. Rutsch
3. Prof. Dr. A. Gamillscheg

Datum der Promotion: 14.09.2007

Abbreviations

A	A wave
AHCM	Apical hypertrophic cardiomyopathy
AVC	Aortic valve closure
AVO	Aortic valve opening
BB	Beta blocker
CCB	Calcium channel blocker
CW	Continuous wave
DMI	Doppler myocardial imaging
E	E wave
ECG	Electrocardiography
EF	Ejection fraction
ET	Ejection time
FHCM	Familial hypertrophic cardiomyopathy
FS	Fractional shortening
FT	Filling time
HCM	Hypertrophic cardiomyopathy
HOCM	Hypertrophic obstructive cardiomyopathy
I/H index	Isovolumic heterovolumic index
IVC/IVCT	Isovolumic contraction time
IVR/IVRT	Isovolumic relaxation time
IVS	Interventricular septum
IVSBI	Interventricular septal basal segment integral
IVSMST	Interventricular septal mid segment strain
LA	Left atrium
LAAA	Left atrial annular (segment) velocity (A wave)
LV	Left ventricle
LVB	Left ventricle basal segment
LVBE	Left ventricle basal segment velocity (E wave)
LVET	Left ventricular ejection time
LVH	Left ventricular hypertrophy
LVID _d	Left ventricle internal dimension in diastole
LVID _s	Left ventricle internal dimension in systole
LVM	Left ventricle mid segment

LVOT	Left ventricular outlet tract
LVOTO	Left ventricular outlet tract obstruction
LVPW	Left ventricle posterior wall
Tei-Index	Myocardial performance index
MRI	Magnetic resonance imaging
MS	Millisecond
PS	Pulmonary stenosis
PW	Pulsed wave
QRS	QRS complex in ECG tracing
RA	Right atrium
RV	Right ventricle
RVMS	Right ventricle mid segment velocity (S wave)
RVBSR	Right ventricle basal strain rate
RVOT	Right ventricular outlet tract
RVOTO	Right ventricular outlet tract obstruction
S wave	Tissue Doppler velocity (S wave)
1/s	strain rate measurement unit
SAM	Systolic anterior movement
SR _S	Strain rate during systole
SR _E	Strain rate in early diastole
SR _A	Strain rate in late diastole
SRI	Strain rate imaging
ε	Strain
TDE	Tissue Doppler echocardiography
TDI	Tissue Doppler imaging
TVI	Tissue velocity imaging

Contents

Abbreviations	3
1 Introduction	8
1.1 Definition	8
1.2 Familial hypertrophic cardiomyopathy (FHCM)	9
1.3 Tissue Doppler imaging (TDI)	10
1.3.1 Strain rate and strain imaging (SRI)	10
1.3.2 Application of tissue Doppler imaging (TDI)	11
1.3.3 Aim of this study	11
2 Material and methods	12
2.1 Study population	12
2.2 Conventional echocardiography	12
2.2.1 Measurement of cardiac cycle time intervals by means of Doppler echocardiography 13	
2.3 Colour myocardial Doppler imaging (CMDI)	14
2.3.1 Tissue Doppler imaging data acquisition	14
2.3.2 Post-processing two-dimensional myocardial colour Doppler velocity data	14
2.3.3 Ventricular myocardial velocity and velocity integral	15
2.3.4 Ventricular myocardial strain rate waves	16
2.3.5 Ventricular myocardial strain	17
2.3.6 Timing of global heart events	18
2.4 Myocardial performance index: TD-derived Tei index	19
2.5 Assessment of atrial function using tissue Doppler imaging	20
2.5.1 Atrial regional myocardial velocity and strain rate	20
2.6 Electrocardiogram	21
2.7 Statistical methods	21

3	Results	22
3.1	Clinical data.....	22
3.1.1	Clinical presentation.....	22
3.2	Conventional echocardiographic findings.....	24
3.3	Electrocardiographic findings	25
3.4	Longitudinal ventricular regional tissue Doppler imaging	25
3.4.1	Velocity, strain rate and strain in the left ventricular wall	25
3.4.2	Velocity, strain rate and strain in the interventricular septum	30
3.4.3	Velocity and strain and strain rate in the right ventricular wall	31
3.5	Regional atrial velocities and strain rates in HCM patients compared to controls	32
3.6	Myocardial performance index and isovolumic intervals	37
4	Discussion	38
4.1	Hypertrophic cardiomyopathy: a rare heterogeneous myocardial disease.....	38
4.2	Hypertrophic cardiomyopathy.....	40
4.2.1	Clinical presentation.....	40
4.2.2	Hypertrophic cardiomyopathy: Treatment.....	40
4.3	Tissue Doppler echocardiography (TDE) and heart function	43
4.3.1	Limitations of conventional echocardiography in quantification of myocardial regional function	43
4.4	Tissue Doppler imaging and cardiac function assessment: LV systolic function.....	44
4.4.1	Qualitatively assessed velocity curves: normal and HCM pattern.....	44
4.4.2	Regional left ventricular longitudinal systolic function and velocity profiles	44
4.5	Regional LV longitudinal systolic function: strain rate and strain curves	45
4.5.1	Tissue Doppler patterns of strain rate: normal and in HCM patients.....	45
4.5.2	Tissue Doppler patterns of strain: normal and in HCM patients.....	46
4.6	Longitudinal ventricular regional strain rate and strain profiles	46

4.7	Regional longitudinal diastolic dysfunction of LV	47
4.7.1	Characteristics of the velocity curves in the interventricular septum: qualitative TDI.	48
4.8	RV function in hypertrophic cardiomyopathy and tissue Doppler imaging	49
4.9	Ventricular interaction.....	50
4.10	Myocardial strain and strain rate measurement: A non-invasive method for quantifying regional myocardial function	51
4.11	Global myocardial function: myocardial performance index (Tei index).....	52
4.12	Doppler derived Tei index as a global parameters of left ventricular systolic and diastolic function.....	52
4.13	Atrial function	53
4.13.1	Longitudinal atrial segmental velocity profiles.....	53
4.13.2	Pattern of atrial strain rates (SR).....	54
4.14	Regional atrial performance in patients with HCM quantified by TD imaging.....	55
5	Summary and conclusions	56
6	Zusammenfassung.....	59
7	References	61
8	Figure/Table index	72
8.1	Figures.....	72
8.2	Tables	73
9	Acknowledgement	74
10	Statement.....	75
11	Curriculum Vitae.....	76

1 Introduction

1.1 Definition

Cardiomyopathies are diseases of the myocardium associated with cardiac dysfunction and they are classified as dilated cardiomyopathy, hypertrophic cardiomyopathy, restrictive cardiomyopathy, and arrhythmogenic right ventricular cardiomyopathy. Hypertrophic cardiomyopathy (HCM) is a genetic disease characterized by cardiac hypertrophy, myocyte disarray, interstitial fibrosis, and left ventricular (LV) dysfunction, with left and/or right ventricular hypertrophy (Fig. 1), which is usually asymmetric and involves the interventricular septum [1] without an identifiable cause. Typically the left ventricular volume is normal or reduced. Systolic pressure gradients in the left and right ventricular outflow tract are common. Depending on the presence or absence of gradient in the LV outflow tract, HCM is classified as obstructive (HOCM) or non-obstructive (HNCM) [2]. The classification of hypertrophic cardiomyopathy is shown in table 1.

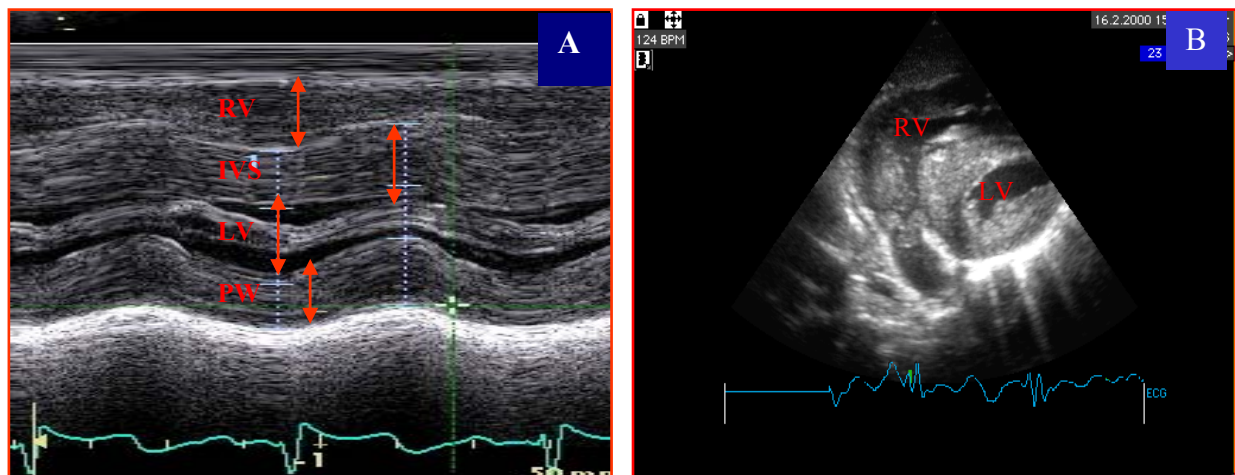


Figure 1: Myocardial hypertrophy of both ventricles in one month old child with HCM (A, B) Parasternal Long (A) and subcostal short (B) axis views showing hypertrophied IVS, left ventricle (LV) and right ventricle (RV) wall in patients with HCM.

Table 1: Classification of hypertrophic cardiomyopathy

- **Morphological:**
 - I Left ventricular involvement
 - 1 asymmetrical hypertrophy
 - a ventricular septal hypertrophy
 - b apical hypertrophy
 - c mid ventricular hypertrophy) or
 - 2 symmetrical (concentric) hypertrophy
 - II Right ventricle involvement
- **Hemodynamically:**
 - 1 Obstructive hypertrophic cardiomyopathy
 - sub aortic obstruction, mid ventricular obstruction
 - 2 non-obstructive
 - normal systolic function
 - impaired systolic function (end stage HCM)
- **Genetically**
 - familial hypertrophic cardiomyopathies

The etiology of HCM is not clear yet but many factors (familial, genetic, viral, infection, mechanical defect, abnormality of muscle structure, abnormality of the electrical conduction within the heart muscle) are involved.

1.2 Familial hypertrophic cardiomyopathy (FHCM)

The most common cause of sudden cardiac death in the young [3], is an autosomal dominant disease caused by mutations in sarcomeric proteins [4]. Because of variable penetrance [4, 5] LVH is absent in a significant number of mutation positive individuals until later in life, such as most patients with FHCM due to myosin-binding protein C mutations [6]. Similarly, individuals with FHCM due to mutations in cardiac Troponin T exhibit minimal LVH, despite having a high incidence of sudden death [5]. The patients with HCM presented with systolic murmur, dyspnoea on exertion and syncopal attack. The manifestation is mainly asymptomatic and at different ages; the left ventricular dysfunction and mitral valve abnormality may lead to clinical symptoms such as exertional dyspnoea, chest pain, syncope, and cardiac arrhythmia and need medical or surgical treatment. The diagnosis of HCM can be established with echocardiography examination and cardiac catheter.

In a minority of HCM patients, however, the impedance to flow occurs at the midventricular level, unrelated to SAM, and is predominantly caused by marked septal hypertrophy coming into contact with a hypercontractile anterolateral LV wall, often with the interposition of the

anterolateral papillary muscle [7, 8], and hypertrophic longitudinal muscle bands on the posterolateral wall of the LV. Midventricular obstruction represents a clinical challenge when associated with severe symptoms, and its treatment is not standardized.

There are important differences from adults in the approach to the diagnosis and management of hypertrophic cardiomyopathy in children and adolescents. The therapy of the patients with HCM includes medical therapy as well as surgical resection (myectomy) of the hypertrophied muscle and pacing therapy and catheter intervention (ASA) alcohol septal ablation in adult, Beta blockers, calcium channel blockers, and anticongestive drugs are mainly the used drugs in treating HCM, hemodynamic changes in HCM that is resistant to medical therapy indicate the surgical intervention (myectomy of the hypertrophied septum) which represents a standard therapeutic option, dual pacing for treatment of HCM is ineffective in children [9]. The transcatheter septal alcohol ablation (Tash) is not indicated in children due to the recurrence of hypertrophy and associated arrhythmia due to scarring [10]. Orthotopic heart transplantation is the last option for those with heart failure and recurrent arrhythmia.

1.3 Tissue Doppler imaging (TDI)

The velocity of myocardial contraction is an established measure of myocardial function [11]. Doppler measurement of myocardial wall velocities (tissue velocity imaging, TVI) was first proposed by Isaaz et al [12]; it is a new technology developed for the evaluation of myocardial motion (longitudinal atrioventricular annular and regional myocardial velocities). The direction and velocity of cardiac movement are evaluated using Doppler techniques specifically designed to record the range of velocities characteristic of the myocardium. After the introduction of a 2-D colour version of this technique (1992), it became the basis of many clinical applications and clinical studies.

1.3.1 Strain rate and strain imaging (SRI)

More recently, Heimdal et al, [13] introduced TD-derived real-time strain rate, from which regional myocardial strain may be derived as the time integral of regional Doppler velocity gradients [14]. Strain rate imaging (SRI) technique added further details to the above items by overcoming some of the limitations of the velocity measurements [15, 16]. Myocardial deformation or strain, a dimensionless description of change in length that reflects deformation of tissue caused by force generation, more directly reflects local myocardial function. Previous data showed that strain was abnormal in the regions related to myocardial infarction or ischemia

[17-19]. However, little was known about the characteristics of strain rate and strain imaging in pediatric patients with hypertrophic cardiomyopathy.

1.3.2 Application of tissue Doppler imaging (TDI)

Potential applications of TDI include improved evaluation of regional and global myocardial function, the differentiation of viable from non-viable myocardium, and enhanced detection of regional wall motion abnormalities during stress echocardiography [20]. Table 2 summarized the current potential applications of TDI [21].

Table 2: Main applications of tissue Doppler imaging in cardiology

Assessment of overall (longitudinal) LV systolic function
Assessment of regional LV systolic function
Diagnosis of myocardial ischemia
Identification of reversible and irreversible myocardial dysfunction
Assessment of global and regional LV diastolic function
Assessment of global and regional systolic and diastolic RV function
Assessment of the function of other cardiac chambers
(e.g., left atrium, right ventricle)
Differential diagnosis between constrictive pericarditis and
restrictive cardiomyopathy
Non-invasive estimation of pressures in cardiac chambers and
pulmonary artery
Localization of accessory conduction pathways
Diagnosis of cardiac transplant rejection

Previous TDI studies have investigated the myocardial dysfunction in patients with different heart diseases, but few of them reported the cardiac dysfunction in hypertrophic cardiomyopathy.

1.3.3 Aim of this study

With the hypothesis of altered global and regional myocardial function in patients with HCM, By using this recent echocardiographic technique, tissue Doppler imaging (TDI), which enables qualitative and quantitative assessment of myocardial tissue velocities, we planned to study the myocardial function in HCM patients; few clinical studies have been done to evaluate the ventricular function by tissue Doppler technique. To our knowledge, atrial function has not yet been evaluated with this new tissue Doppler technique, especially in patients with HCM. Thus another aim of this study was to determine regional atrial function non-invasively and quantitatively, using the TDI myocardial velocity and strain rate parameters.

Hypothesis: we suggested an alteration of global and regional myocardial function in patients with HCM .

2 Material and methods

2.1 Study population

Our study population consisted of 20 patients (9 female, 11 male, age 18.6 (8.8) years) referred to the German Heart Institute Berlin during the period from 1998 till April 2003 with a diagnosis of hypertrophic cardiomyopathy. They were evaluated regarding past medical history, and the initial clinical symptoms and signs and the family history of heart disease or HCM or genetic diseases were recorded. Beside drug therapy, age at onset of the symptoms, age at any intervention and the interval between the initial diagnosis and intervention were recorded. Associated heart defects and other syndromes were noted, using non-invasive procedures (echocardiography, Doppler, ECG) and invasive diagnostic tools and therapy. The diagnosis of HCM is based on 2-D echocardiography, Doppler and cardiac catheter findings of hypertrophy of cardiac muscle and significant intraventricular obstruction and pressure gradients. The novel non-invasive tissue Doppler imaging of the LV, RV and both atria was performed to evaluate the diastolic dysfunction of the LV and to evaluate the extent to which atrial function is affected. The control group consisted of 20 (10 female) age-matched healthy subjects. The patients were in NYHA Class I-II.

2.2 Conventional echocardiography

Examination was carried out using a 2.5 to 3.5 MHz transducer interfaced with the Vingmed System V ultrasound system (GE Vingmed, Horten, Norway). All patients underwent standard transthoracic imaging at rest of the heart and great vessels, which was performed in left lateral decubitus position. Initially, routine diagnostic imaging including M-mode as well as colour and Doppler measurement of blood flow hemodynamics was performed. Simultaneous ECG recording was done in all patients and controls during the echocardiographic examination.

In parasternal long axis; standard M-mode imaging of the LV at the mitral valve was performed. The thickness of the interventricular septum (IVS) and the posterior wall of the left ventricle (PW), left ventricular internal dimension (LVID) in end-diastole and end-systole, fractional shortening (FS) and ejection fraction (EF) were recorded. Presence or absence of SAM phenomenon was documented. The colour flow mapping which is performed in each plane to detect flow disturbances in the left ventricular outlet tract (LVOT) or right ventricular outlet tract (RVOT), intracavity obstructions and valvular or septum defects was carried out. In apical four-chamber view; the LV outlet tract was imaged and the outflow velocity profiles were recorded

with Doppler sample placed just below the aortic annulus. Blood flow acceleration were measured first by pulsed wave (PW) Doppler imaging to confirm flow disturbance and then by the continuous wave (CW) Doppler imaging to assess the peak flow velocity and to quantify the pressure gradient. The usual size of the pulsed Doppler (PW) gate was 1.5 mm and the filter was set at 100 Hz for optimal acquisition of the Doppler signals. All measurements were stored digitally for subsequent offline data analysis. The average value of each parameter was calculated in 5 consecutive heartbeats. The mitral and tricuspid valve inflow velocity profiles were recorded with the Doppler sample placed at the tip of the mitral and tricuspid valve, respectively. The rapid diastolic filling flow wave (E wave) and atrial contraction wave (A wave) were analyzed. The peak velocities of E and A wave were measured.

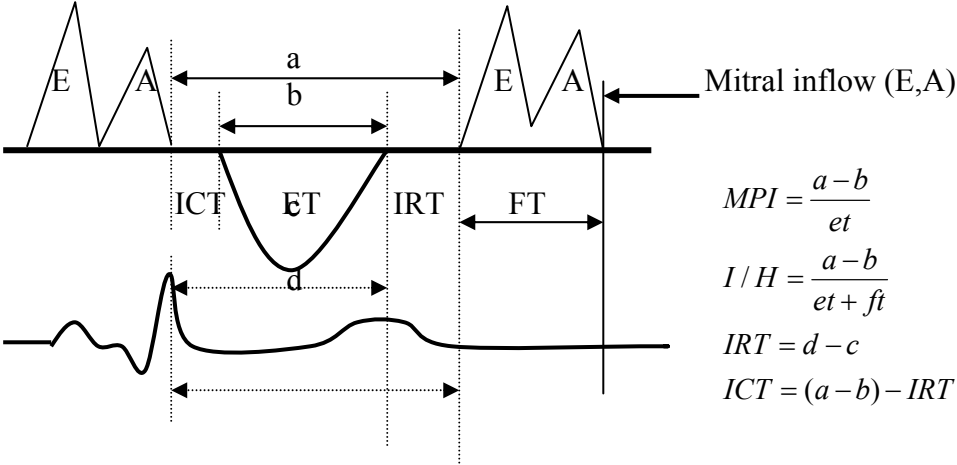


Figure 2: Calculation of cardiac cycles intervals.

E & A mitral inflow waves, ICT= isovolumic contraction time, IRT= isovolumic relaxation time, FT= filling time , I/H: isovolumic heterovolumic index.

2.2.1 Measurement of cardiac cycle time intervals by means of Doppler echocardiography

Figure 2 shows the standard cardiac cycle time intervals that were estimated by Doppler echocardiography. The a value, the time interval from the cessation to the subsequent opening of the mitral valve inflow and ejection time (b value) derived from Left ventricular outflow Doppler velocity profile were measured.

The ejection time is the entire time interval of the aortic valve systolic Doppler flow signal [22], the c value is the time interval from the peak R wave (first positive deflection after the P wave on the ECG to the end of the aortic valve velocity signal) and the d value is the time interval from

peak R wave on the ECG to the subsequent mitral valve opening. The myocardial performance index (Tei index) was calculated according to the equation $\text{Tei index} = (a-b) / b$ [23].

The minimal ventricular isovolumic relaxation time, the time interval between the cessation of left ventricular ejection and the onset of the left ventricular filling, can be calculated by subtracting the c value from the d value [24, 25]. The left ventricular isovolumic contraction time, the time interval between cessation of left ventricular filling and the onset of left ventricular ejection can be calculated according to the formula: $\text{isovolumic contraction time} = (a-b) - \text{isovolumic relaxation time}$ [25] (Fig 2). The same parameters can now be derived by TDI technique as will be discussed under timing of global heart events.

2.3 Colour myocardial Doppler imaging (CMDI)

2.3.1 Tissue Doppler imaging data acquisition

After the diagnostic standard transthoracic echocardiography examination was completed, the setting of the echocardiographic was switched to the application of TDI with patient in the same position with simultaneous ECG recording. An apical 4-chamber view was obtained with colour coded 2-D method, including both ventricles and both atria. The echocardiography beam was aligned parallel with the walls of each myocardial segment, thus minimizing the effect of the insonation ($< 30^\circ$). A single cine-loop for LV and LA free wall, RV and RA free wall and IVS and IAS wall, respectively, was obtained. This technique measures mean velocities (not peak) with both high temporal (130 ± 20 frames/s) and high spatial resolution in the axial direction. The cine-loop with 3 heart cycles was transferred to Echo Pac and recorded digitally for offline processing. The same technique was performed for the controls.

2.3.2 Post-processing two-dimensional myocardial colour Doppler velocity data

At the special workstation designed for offline measurement of the collected tissue Doppler data we subsequently analyzed the data for different systolic and diastolic parameters of TDI (velocities, integral, strain, strain rate) and calculated the different indices in the patients and controls. The evaluation of the regional atrial function was carried out with the same principles as for ventricular regional function using velocity curves and strain rate imaging. All analyses were performed at a computer workstation with customised software (TVI; GE Vingmed, Echo Pac 6.3.6, GE Vingmed, Horten, Norway) and reported as the average of the 3 consecutive cardiac cycles. Regions of interest were placed at the basal and mid myocardial segments of each wall (IVS, RV and LV free wall) and at the corresponding region of interest for the atrial walls:

annular and mid segments. A tagging technique was used to control the position of the sample volume within the ventricular and particularly within the atrial wall. The maximal and minimal values at the time velocity and strain rate curves were tagged and the simultaneous position of the sample volume was controlled to remain within the myocardial wall region.

2.3.3 Ventricular myocardial velocity and velocity integral

In the patients and controls, at the basal and mid segment of the LV, RV free wall, and IVS, the velocities were recorded by applying 3x3 pixel sample. The mean regional velocity positive wave during systole (S wave), the early diastolic negative wave (E wave) and the late diastolic negative wave (A wave) were measured and their values in cm/s were recorded (Fig. 3a and b). The time from the first positive deflection (R) on the simultaneously recorded ECG to the peak of the S, E and A waves respectively were measured and its value in ms was recorded. The recorded velocities in patients with HCM were compared to the corresponding values in the controls.

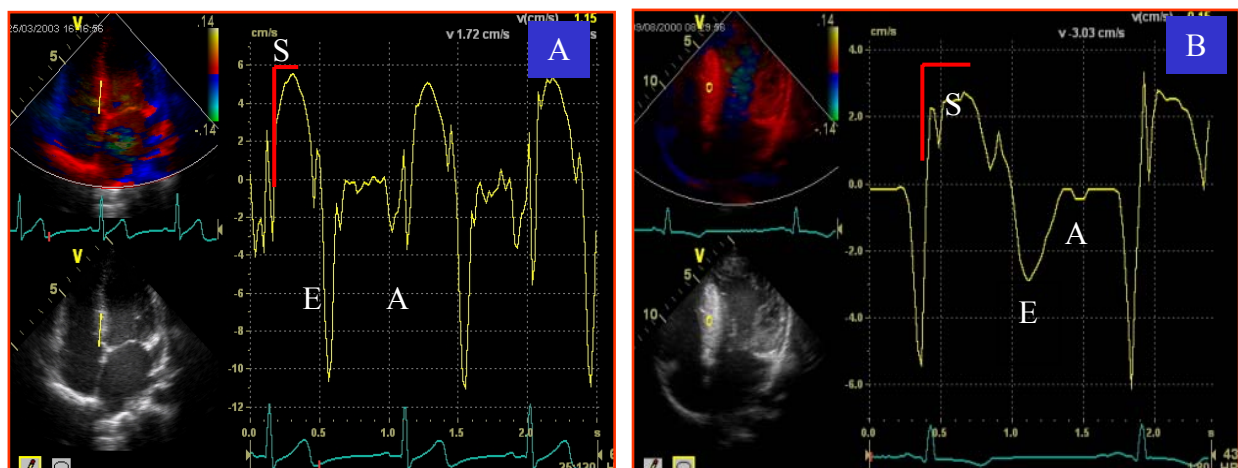


Figure 3: The pattern of myocardial longitudinal velocity deformations. systolic (S), early diastolic (E) and late diastolic (A) waves of the mid segments of interventricular septum in controls (A) and HCM patients (B)

Myocardial displacement (the distance the myocardium moves during systole in cm) was recorded and its peak time, the time from R wave on the ECG to the peak of the myocardial integral, and diastolic time (time at the end of cardiac cycles when the curve returns to zero value) in the two groups were recorded (Fig. 4).

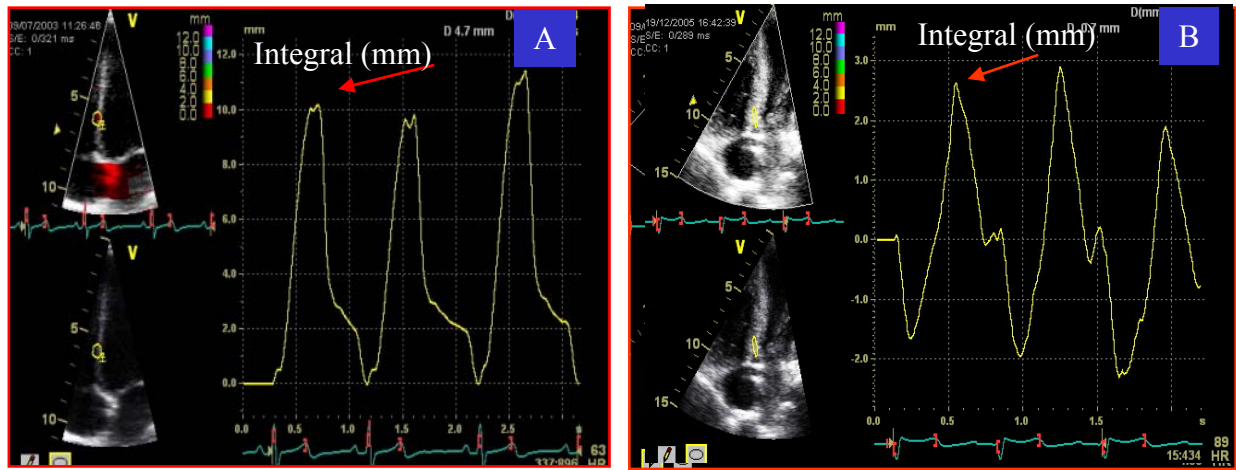


Figure 4: Velocity integral (mm) at mid IVS-wall in controls (A) and patients with HCM (B)

2.3.4 Ventricular myocardial strain rate waves

Accordingly the strain rate curve of the LV and RV free walls and IVS at the same points with computation distance of 9.7 mm in longitudinal direction of the patients and controls were measured; the negative wave during systole (S wave) and the positive waves (E and A waves) during early and late diastole were measured and their value in 1/s recorded (Fig. 5).

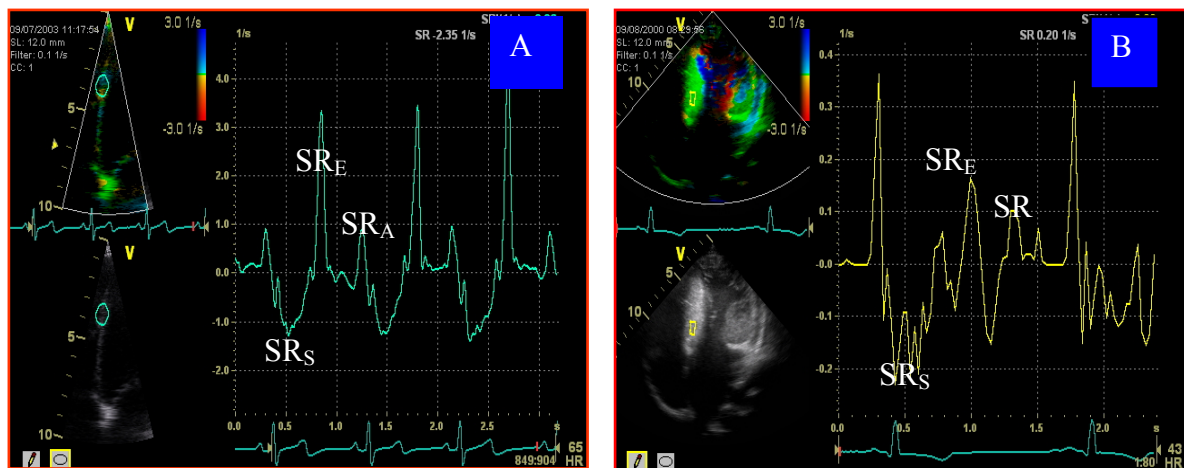


Figure 5: Pattern of strain rate curve at the IVS wall in controls (A) and in HCM patients (B) Show negative systolic (SR_S) and diastolic positive early (SR_E) and late (SR_A) strain rate waves.

2.3.5 Ventricular myocardial strain

In the patients and controls, the strain of the examined part was estimated with computation distance of 9.7 mm in longitudinal direction and at the same sites, and the negative wave (strain) maximal value in percent (%) and the time required by the myocardium to achieve this maximum percentage of deformation were recorded.

Myocardial deformation was assessed in the septal and lateral walls (apical 4-chamber view). The end point of the T wave of the electrocardiogram was used as the reference point of end systole (Figs. 6, 7). We compared the strain in patients with HCM to controls and correlated the values to other parameters.

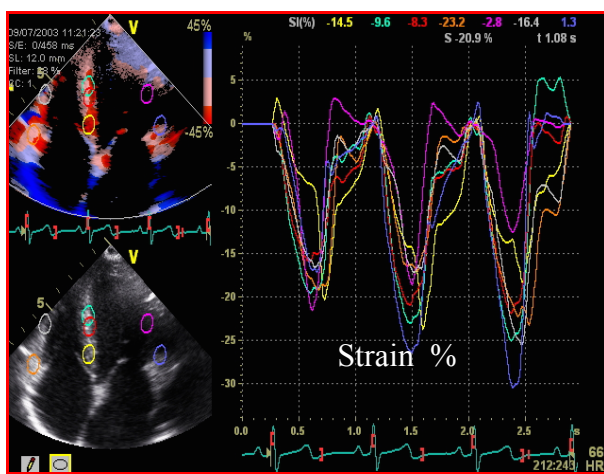


Figure 6: An example of myocardial strain pattern in normal subject

Strain in basal and mid segments of LV, IVS and RV were always negative during systole and showed parallel changes in healthy individuals

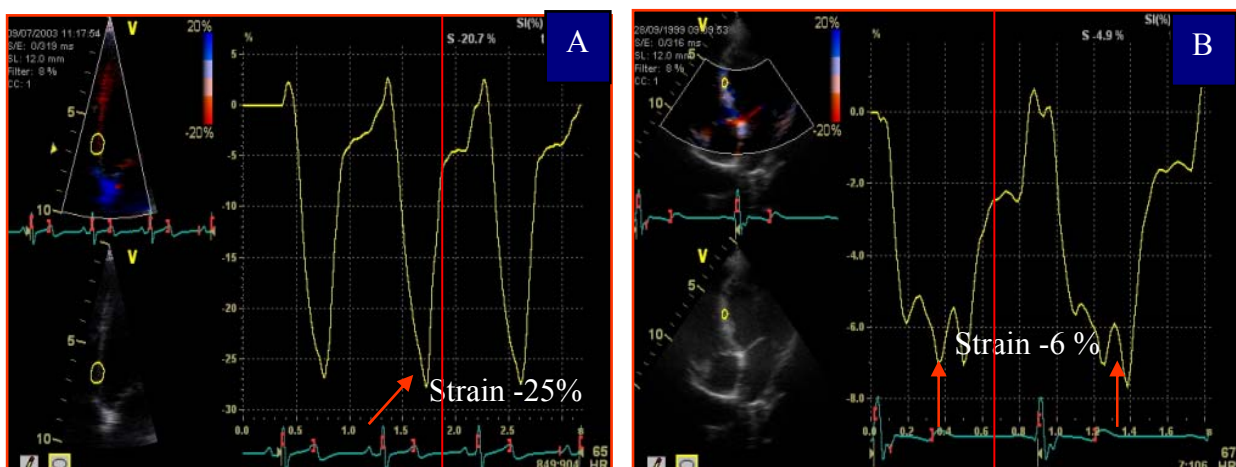


Figure 7: Pattern of normal strain in IVS of controls(A) and abnormal strain at IVS in HCM patients (B)

2.3.6 Timing of global heart events

It is important to time both global and local mechanical events when attempting to compare global with regional function. Because the interventricular septum is of particular interest when the timing of events is studied [26-28] we used the septal basal colour Doppler tissue velocity (unprocessed velocity curve) to time the opening and closure of aortic valve for each cardiac cycle (Fig. 8b). Both mechanical events induce a clearly identifiable rapid change in the basal septal velocity curves which correlates with the timing of the rapid upstroke and peak negative left ventricular dp/dt, respectively [29, 30]. The timing of mitral valve events was obtained using an anatomic greyscale M-mode cursor positioned at the level of the mitral valve leaflets (Fig. 8a), [31].

With this method it was possible to measure the different cardiac cycle intervals: isovolumic contraction time (IVCT), ejection time (ET), isovolumic relaxation time (IVRT), and filling time (FT), and myocardial performance index was calculated according to the formula $IVCT+IVRT / ET$ (Figs. 8a, 8b, 9).

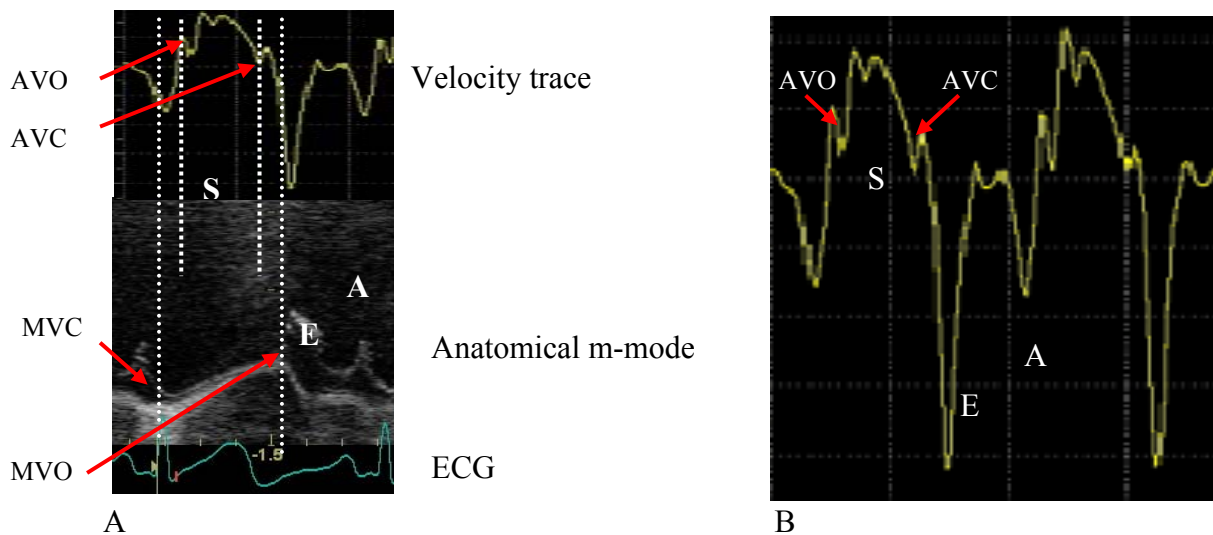


Figure 8: Tissue Doppler and cardiac cycle intervals.

A- Cardiac cycle events; the longitudinal velocity pattern at mid IVS-segment in normal subject. With Systolic (S) and early (E) and late diastolic (A) waves. **B-** time of aortic valve opening (AVO) and closure (AVC) on the velocity curve.

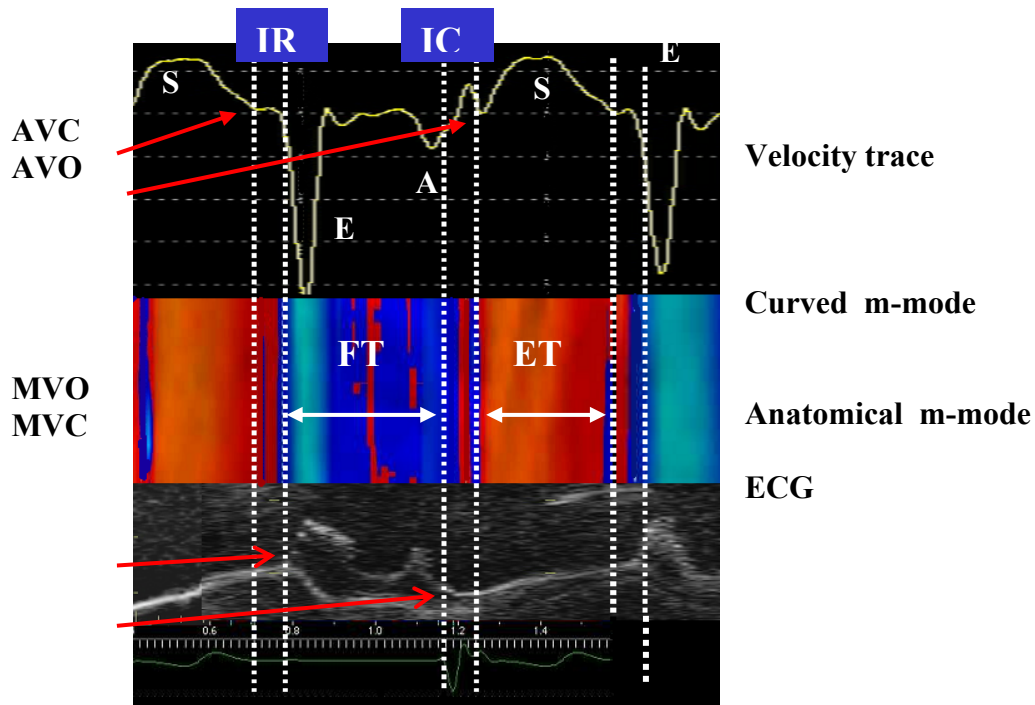


Figure 9: Cardiac cycle intervals timing presented according to changes with basal septal velocity trace, colour curved M-mode tissue Doppler and anatomical M-mode velocity trace.

MVC: mitral valve closure, MVO: mitral valve opening, AVC: aortic valve closure, AVO: aortic valve opening, IC: isovolumic contraction time, IR: isovolumic relaxation time, FT: filling time, ET: ejection time. S: systolic velocity, E and A: early and late diastolic velocity.

2.4 Myocardial performance index: TD-derived Tei index

Myocardial performance index (Tei index) is defined as the sum of isovolumic contraction and relaxation times divided by ventricular ejection time. It is correlated to the pulsed Doppler Tei index, which reflecting the global cardiac function [32, 33]. From the tissue Doppler image (Figs. 8 and 9), we derive the intervals of isovolumic contraction time (ICT), isovolumic relaxation time (IRT), and the ejection time (ET). Intervals measured are depicted in Figure 9. The filling time (FT) of the left ventricle, from opening to closure of the mitral valve (MV) was measured from the greyscale M-mode as mentioned above. Tei Index of the left ventricle was calculated using the formula: $\text{Tei index} = (\text{ICT} + \text{IRT}) / \text{ET}$. Additionally, we determined the isovolumic/heterovolumic time ratio (I/H index = $(\text{ICT} + \text{IRT}) / (\text{ET} + \text{FT})$), which expresses the time taken by the myocardium to generate and decrease LV pressure without moving blood.

2.5 Assessment of atrial function using tissue Doppler imaging

From the apical 4-chamber view, measurements were made from 4 segments of the left atrium (1: septal annular segment; 2: septal mid segment; 3: lateral mid segment; 4: lateral annular segment) and 2 segments of the right atrium (5: lateral annular segment; 6: lateral mid RA segment) (Fig. 10). As the atrium is thin-walled, we measured segmental velocities using the traditional 9 x 9 pixel size described in the literature [34], and a tissue velocity profile throughout the cardiac cycle was displayed in each sample location (Figs. 11a and b). The mean peak velocity of atrial contraction was measured in each segment as an average of 3 beats.

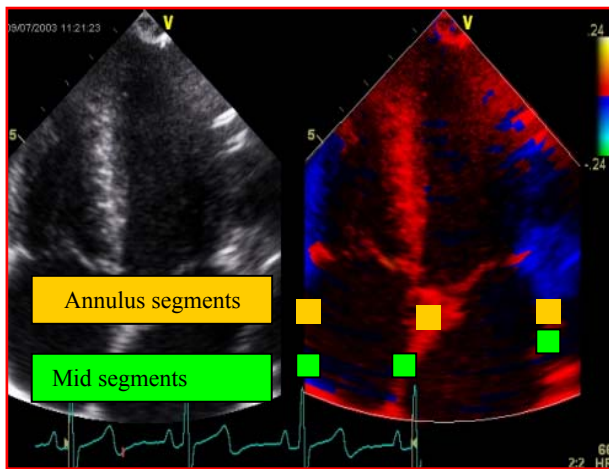


Figure 10: Sites of velocity samples at the annular and mid segments of the atrial walls

2.5.1 Atrial regional myocardial velocity and strain rate

In the patients, at the region of interest as stated above for both atria, the systolic S wave and diastolic E and A wave magnitude were estimated and their value in cm/s was recorded (Fig. 11a). Similarly, The SR_S (systole), SR_E (early diastole) and SR_A (atrial contraction) waves were recorded (Fig. 11b). The left atrial wave SR_A reflects the regional atrial deformation and may provide information on regional contractile function. The values measured were compared to those of controls, and correlated to other parameters.

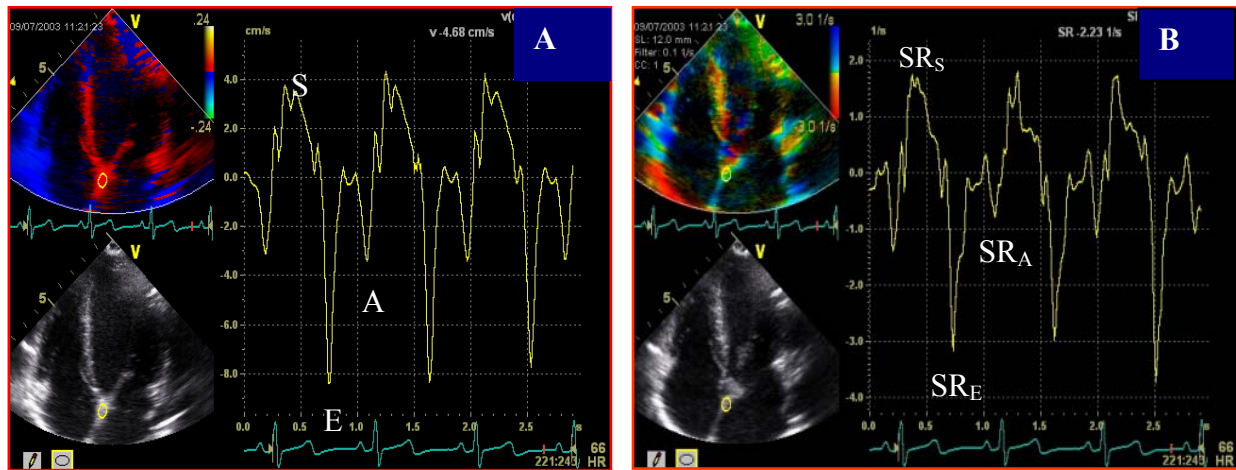


Figure 11: Pattern of atrial regional velocity (A) and strain rate at IAS annular segments in controls (B)

S: systolic velocity, E,A: early and late diastolic velocity, SR_S: systolic strain rate, SR_E, SR_A: diastolic strain rate in early and late diastolic phase

2.6 Electrocardiogram

All patients had a 12 lead surface ECG performed with a Siemens recorder (Siemens, Erlangen, Germany) at a speed of 25mm/sec, and 1mv/cm standardization. The ventricular hypertrophy was estimated by Sokolow and Lyon method by summation of S and R waves in V2 and V5 respectively. If the value is > 35 mm, the LV is hypertrophied.

2.7 Statistical methods

Data analysis was done with the SPSS 11 statistic programme. Data are expressed as mean \pm SD. Assessment of the differences between the means of the measured parameters of the patient and control groups was generally done by applying the nonparametric Mann-Whitney test for two unpaired groups and paired t-test within the group were performed. For the analysis of correlation the parametric Pearson correlation and nonparametric Spearman rank correlation were performed. A difference was considered significant at $p < 0.05$.

3 Results

3.1 Clinical data

The mean age of patients at time of examination was 18.6 (8.8) years, all patients were in good physical health with New York Heart Association (NYHA) functional class I-II, the weight and height at examination, blood pressure and other characteristics are summarized in Table 3.

Table 3: Patients' characteristics (n = 20)

Parameter	HCM patients	Control subjects	P
	Mean \pm SD	Mean \pm SD	
Age (years)	18.60 \pm 8.80	19.48 \pm 9.30	0.22
Male gender	11	10	--
Heart rate (bpm)	79.8 \pm 17	74.7 8 \pm 10	0.22
Body weight (kg)	56.98 \pm 23.90	61.68 \pm 19.9	0.6
Height (cm)	160 \pm 29.50	159 \pm 34.60	0.37
systolic blood pressure (mmHg)	113 \pm 13.00	111 \pm 10.34	0.29
diastolic blood pressure (mmHg)	57 \pm 10.30	56 \pm 9.37	0.62
Age at time of initial diagnosis (months)	64.30 \pm 81.40	--	--
Age at intervention (months)	136.40 \pm 101.60	--	--
Interval from diagnosis to intervention (months)	93.90 \pm 42.50	--	--

3.1.1 Clinical presentation

The clinical manifestations in our patients are shown in Figure 12. In our series 15% of patients were diagnosed in the neonatal period, 50% before starting school and 95 % before reaching the age of 13 (Fig. 13). In 20% of our patients, such clinical syndromes were diagnosed: about 5% with Beckwith Wiedemann syndrome, 5% with Noonan syndrome, 5% with mucopolysaccharidosis and 5% with renal dysplasia (Fig. 14). Important associated cardiac defects such as septal defects and valvular lesions have also been

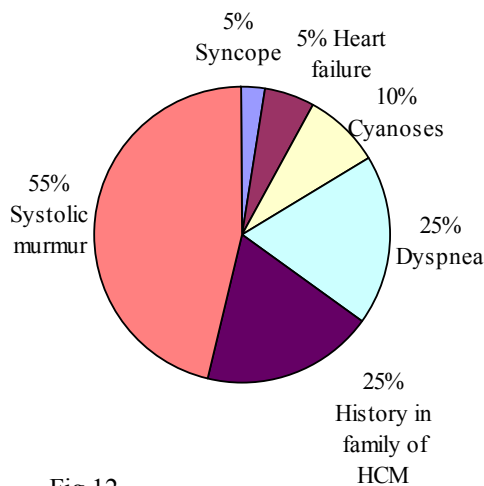


Fig 12

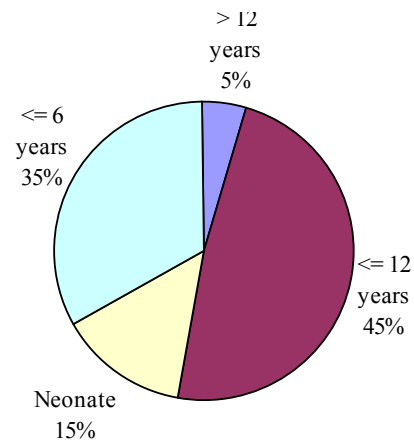


Fig 13

Figure 12: Distribution of clinical manifestations in the paediatric patients studied.

Figure 13: The distribution of patient ages at the time of initial manifestation of HCM.

Almost 50% of cases first manifested in childhood.

documented; where about 10% of our cases had a ventricular septal defect. Echocardiographic examination revealed that 65% have mild mitral insufficiency (MI) and 50% the SAM phenomena. Valvular lesions such as mild aortic and pulmonary stenosis are found in association with some clinical syndromes (Figs. 14, 15).

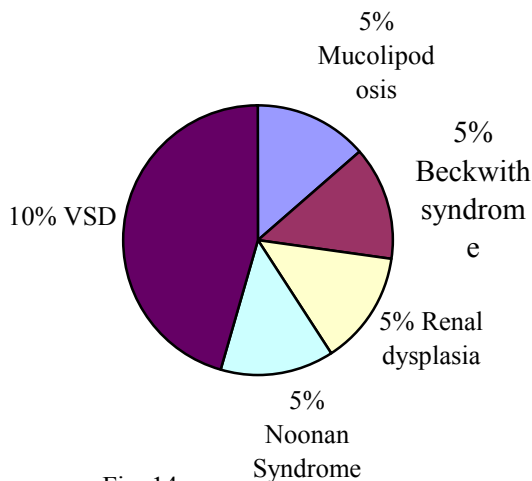


Fig. 14

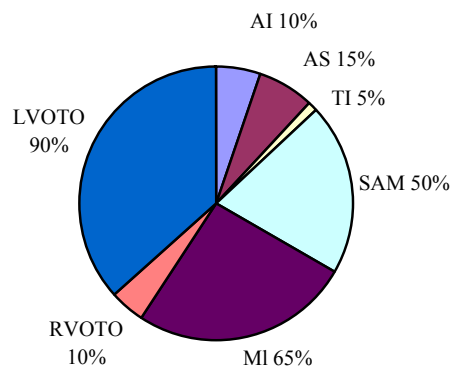


Fig. 15

Figure 14: Abnormal cardiac and non-cardiac conditions associated with hypertrophic cardiomyopathy

Figure 15: Abnormal echocardiographic findings in patients with HCM.

AI: aortic insufficiency, AS: aortic stenosis, SAM: systolic anterior movement, MI: mitral insufficiency, RVOTO: right ventricular outlet obstruction, LVOT: left ventricular outlet obstruction.

3.2 Conventional echocardiographic findings

The echocardiographic examination (Table 4) revealed interventricular septum hypertrophy and intraventricular obstruction, with turbulent flow and a significant pressure gradient across the left ventricular outflow tract (LVOT). Doppler examination showed that 90% of patients had turbulent flow in the LVOT, PW and CW examination measured the maximal velocity value in the LVOT as ranging from 1 to 4.7 m/s, and calculated pressure gradient across the LVOT as ranged from 12 to 170 mmHg, with a mean of 64.6 ± 42 mmHg. Ten percent of the patients had gradients of less than 30 mmHg across the LVOT. A further, 10% of the study population had additional right ventricular outflow tract (RVOT) obstruction due to IVS hypertrophy with a gradient of 25-90 mmHg, mean 46 ± 28 mmHg. Sixty-five percent of the patients had mild to moderate mitral valve insufficiency and 50% systolic anterior movement of the mitral valve leaflet (SAM phenomenon). About 20 percent of those with mitral insufficiency have SAM. Systolic global cardiac function of the hypertrophied cardiac muscle, with EF 73 ± 17 % and FS 45 ± 12 % was normal. Conventional echocardiography except the wall thickness provides no quantitative information on abnormal systolic and diastolic function.

Table 4: Echocardiographic findings Echocardiographic findings of 20 patients with HCM in comparison to 20 controls.

Echocardiographic findings	Patients (20) Mean \pm SD	Controls (20) Mean \pm SD	P
EF (%)	73.80 \pm 17.5	72.90 \pm 14	0.22
FS (%)	45.60 \pm 12.6	43.70 \pm 10	0.41
LVIDd (mm)	37.30 \pm 3.40	39.80 \pm 2.9	0.32
LVIDs (mm)	26.10 \pm 0.91	27.21 \pm 0.72	0.31
RVIDd, (mm)	16.02 \pm 0.30	17.20 \pm 0.12	0.12
RVIDs mm	8.30 \pm 0.12	1.00 \pm 0.13	0.35
IVSd thickness (mm)	18.70 \pm 0.72	15.21 \pm 0.45	0.001
PWd (mm)	9.90 \pm 0.31	9.70 \pm 0.43	0.61
IVSs/PWs (m/s)	1.40 \pm 0.75	1.01 \pm 0.11	0.01
LVOT Vmax (m/s)	3.10 \pm 1.10	1.20 \pm 0.40	0.001
LVOT gradient (mmHg)	64.60 \pm 42	9.40 \pm 0.30	0.001
RVOT gradient (mmHg)	46.00 \pm 27.8	7.40 \pm 5.30	0.021
Mitral Doppler inflow E wave (m/s)	0.88 \pm 0.30	0.93 \pm 0.16	0.08
Mitral Doppler inflow A wave (m/s)	0.58 \pm 0.20	0.62 \pm 0.14	0.09
E/A at mitral valve	1.52 \pm 6.3	1.50 \pm 0.20	0.12
Tricuspid Doppler inflow E wave (m/s)	0.52 \pm 0.13	0.55 \pm 0.10	0.08
Tricuspid Doppler inflow A wave (m/s)	0.45 \pm 0.13	0.49 \pm 0.10	0.07
E/A at tricuspid valve	1.15 \pm 1.01	1.12 \pm 1.03	0.32
Cycle length (ms)	801.8 \pm 246	817.3 \pm 113	0.22

EF= ejection fraction, SF= shortening fraction, LVIDd,s/ RVIDd,s= left /right ventricular internal diameter in diastole and systole, LVOT= left ventricular outflow tract, IVS = interventricular septum, PW= posterior wall, E/A = ratio of mitral or tricuspid flow in early and late diastole

3.3 Electrocardiographic findings

The electrocardiogram showed mostly left ventricular hypertrophy, right ventricular hypertrophy, and biventricular hypertrophy changes.

3.4 Longitudinal ventricular regional tissue Doppler imaging

3.4.1 Velocity, strain rate and strain in the left ventricular wall

The velocity curves of the LV free wall showed a significant reduction in the mean value of the S, E and A wave at the base and midsegments in comparison to the controls. For details of velocity distribution see Table 5.

Table 5: Comparison between the longitudinal ventricular segmental velocities (cm/s) in HCM patients (n=20) and controls (n=20), (mean \pm SD)

Parameters	Velocity (mean \pm SD)								
	S			E			A		
	HCM	controls	P	HCM	controls	P	HCM	controls	P
LV basal	5.14 \pm 2.18	7.74 \pm 1.31	0.001	6.63 \pm 3.65	10.75 \pm 3.23	0.01	2.93 \pm 1.84	4.98 \pm 1.63	0.047
LV middle	3.88 \pm 1.49	5.69 \pm 1.47	0.014	4.57 \pm 2.74	8.51 \pm 3.13	0.002	1.20 \pm 1.00	3.26 \pm 1.25	0.001
IVS basal	4.71 \pm 1.44	6.99 \pm 1.33	< 0.001	4.44 \pm 2.46	10.17 \pm 1.09	< 0.001	3.69 \pm 1.61	6.12 \pm 1.96	0.005
IVS middle	3.17 \pm 1.35	4.53 \pm 1.37	0.041	3.46 \pm 2.13	8.69 \pm 1.53	< 0.001	3.03 \pm 1.49	3.43 \pm 1.79	0.849
RV basal	8.38 \pm 3.02	10.50 \pm 1.66	0.047	7.50 \pm 3.64	10.27 \pm 3.38	0.060	7.62 \pm 2.77	6.64 \pm 1.98	0.280
RV middle	4.46 \pm 3.34	8.37 \pm 1.56	0.005	4.02 \pm 3.18	9.82 \pm 1.99	< 0.001	4.26 \pm 3.55	5.89 \pm 3.10	0.135

LV basal and LV middle: LV basal & middle segment, IVS basal & IVS middle: interventricular basal and mid segment, RV basal and RV middle: right ventricular basal and mid segment, S: systolic velocity, E, A: early and late diastolic velocity

Strain rate at the basal LV free wall segment showed significant reduction in the systolic phase in patients with HCM with mean SR_S 1.42 ± 1.00 (1/s) versus 1.98 ± 1.11 (1/s) in controls ($p = 0.04$) and stronger paradoxical strain rate (SR_S) change at mid segment (1.52 ± 1.21 (1/s) in HCM versus 1.23 ± 1.36 (1/s) in controls, $p < 0.001$). There was no significant difference between the HCM patients and controls for SR_E and SR_A waves at basal or mid segment of the LV free wall (Fig. 16).

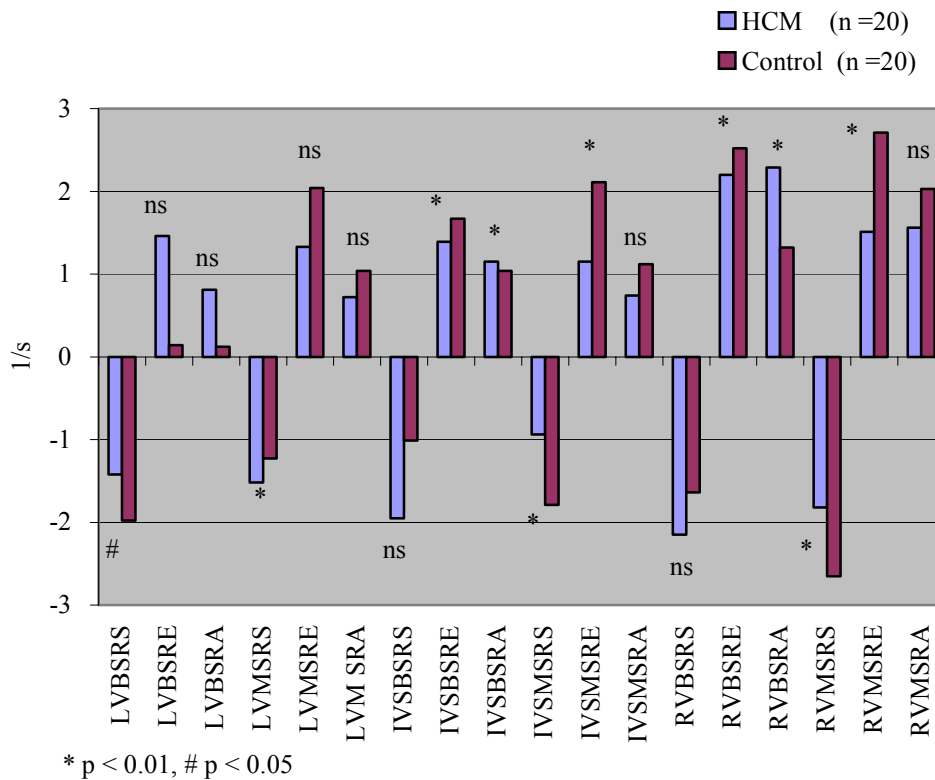


Figure 16: Comparison of ventricular regional strain rate values at different points of myocardial segments between HCM and controls

LVBSRS= left ventricular basal systolic strain rate S, LVBSRE= left ventricular basal strain rate in early diastolic E, LVBSRA= left ventricular basal strain rate in late diastolic A, LVMSRS= left ventricular mid systolic Strain rate S, LVMSRE= left ventricular mid early diastolic strain rate E, LVMSRA= left ventricular mid late diastolic strain rate A, IVSBSRS= interventricular septum basal systolic strain rate S, IVSBSRE= interventricular septum basal early diastolic strain rate E, IVSBSRA= interventricular septum basal late diastolic strain rate A, IVSMSRS= interventricular septum mid systolic strain rate S, IVSMSRE= interventricular septum mid early diastolic strain rate E, IVSMSRA= interventricular septum mid late diastolic strain rate A, RVBSRS= right ventricular basal systolic strain rate S, RVBSRE= right ventricular basal early diastolic strain rate E, RVBSRA= right ventricular basal late diastolic strain rate A, RVMSRS=right ventricular mid systolic strain rate S, RVMSRE=right ventricular mid early diastolic strain rate E, RVMA= right ventricular mid late diastolic strain rate A.

The time to peak (TTP), the time in milliseconds taken by each wave to reach its peak, of the consecutive velocity waves (S, E, A) was significantly delayed in HCM patients in comparison to controls. The systolic peak of myocardial velocity is significantly delayed at the basal and mid segments of the LV, septal wall and RV mid segment (Fig. 17).

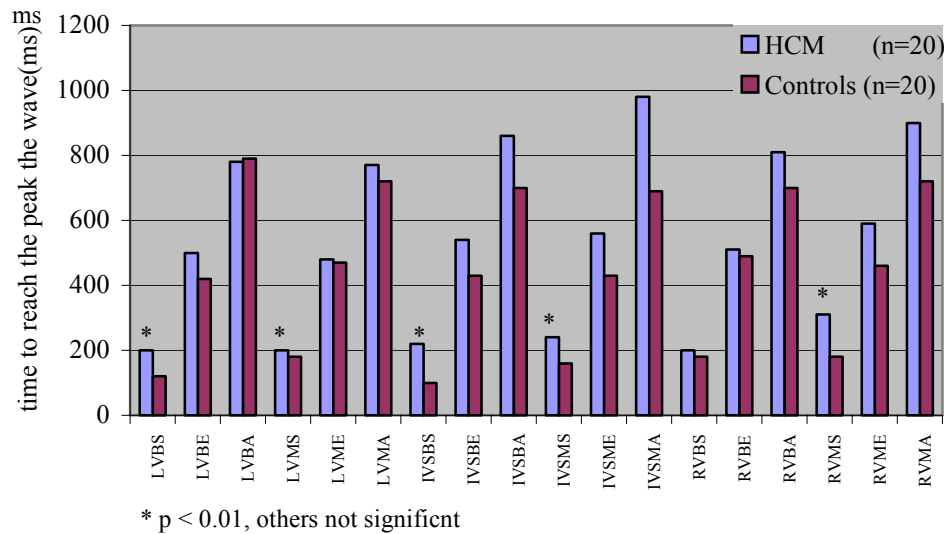
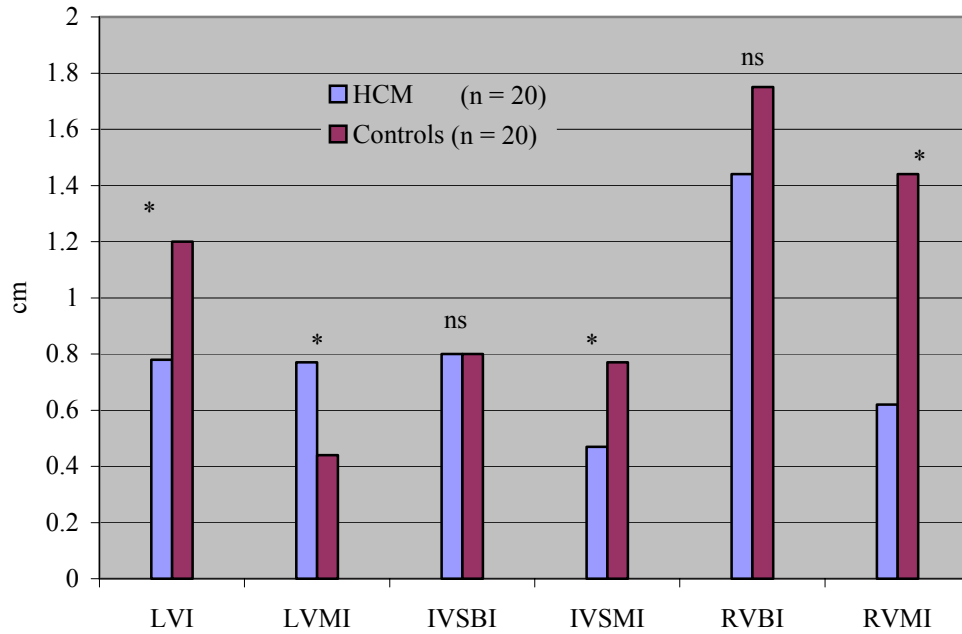


Figure 17: Significant delay of systolic (s) myocardial velocities to reach its peak in HCM patients at different myocardial segments in comparison to controls

LVBS= left ventricular basal systolic velocity , LVBE= left ventricular basal early diastolic velocity, LVBA= left ventricular basal diastolic velocity, LVMS= left ventricular mid systolic, LVME= left ventricular mid diastolic velocity, LVMA= left ventricular mid diastolic velocity, IVSBS= interventricular septum basal systolic, IVSBE= interventricular septum basal diastolic, IVSBA= interventricular septum basal diastolic, IVSMS= interventricular septum mid systolic velocity, IVSME= interventricular septum mid diastolic velocity, IVSMA= interventricular septum mid diastolic, RVBS= right ventricular basal systolic velocity, RVBE= right ventricular basal early diastolic velocity, RVBA= right ventricular basal late diastolic velocity, RVMS= right ventricular mid systolic velocity, RVME= right ventricular mid early diastolic velocity, RVMA= right ventricular mid early diastolic velocity.

A significant difference between the velocity integral in HCM and controls at the base of the LV free wall (mean 0.76 ± 0.34 cm versus 1.2 ± 0.35 cm, $p = 0.001$), LV mid segment ($p = 0.02$), IVS mid segment ($p = 0.008$), and RV mid segment ($p = 0.001$) is shown in Figure 18.



* p < 0.01, ns: not significant

Figure 18: The longitudinal ventricular velocity integral (displacement in cm) was significantly reduced in patients with HCM.

LVBI= left ventricular basal integral, LVMI= left ventricular mid integral, IVSBI= interventricular septum basal integral, IVSMI= interventricular septum mid integral, RVBI= right ventricular basal integral, RVMI= right ventricular mid integral

The regional strain analysis showed no significant difference at the basal and mid point of the LV free wall in patients with HCM in comparison to the control group (Table 6). The strain in the LV mid segment showed a significant positive correlation to the Tei index ($r = 0.6$, $p = 0.03$) in HCM patients but not in controls and also associated with the strain of the RV basal segment ($r = 0.9$, $p = 0.02$) in patients and in controls ($r = 0.8$, $p = 0.002$).

Table 6: Comparison between the strain in HCM and controls at different myocardial segments

Parameters %	HCM (n=20)	Controls (n=20)	P
	Mean \pm SD	Mean \pm SD	
LVB strain	13.99 \pm 7.29	19.10 \pm 8.67	0.212
LVM strain	16.10 \pm 8.90	17.77 \pm 9.45	0.790
IVSB strain	17.58 \pm 8.10	24.50 \pm 7.80	0.034
IVSM strain	8.80 \pm 4.60	23.53 \pm 6.60	0.001
RVB strain	24.90 \pm 14.30	19.40 \pm 5.70	0.368
RVM strain	17.40 \pm 10.30	28.90 \pm 10.40	0.007

LVB/LVM= left ventricular basal and mid segment, IVSB/IVSM= interventricular basal and mid segment, RVB/RVM= right ventricular basal and mid segment.

3.4.2 Velocity, strain rate and strain in the interventricular septum

In the interventricular septum, the regional tissue Doppler velocity, strain rate and strain values at the basal and mid segments revealed a significant reduction in patients with HCM in comparison to controls. Strain rate E /A ratio at basal or mid septal segment was insignificant, respectively, ($p = 0.97$, $p = 0.31$). In patients with HCM the strain at the basal segment of the IVS is positively correlated to the I/h index ($r = 0.6$, $p = 0.02$) but not in controls ($r = 0.1$, ns).

The E/A ratio is significantly reduced at septal mid segment ($p = < 0.001$). There was a significant difference between strain in patients with HCM and controls (8.8 ± 4.6 versus 23.53 ± 6.6 %, $p = 0.001$). Altered regional contractile function according to regional strain and diastolic strain rate was found in the basal and mid septal segment.

The summary of tissue Doppler assessment of the hypertrophied interventricular septum in our study is provided in Table 7.

Table 7: Tissue Doppler parameters in interventricular septum of HCM and control patients

Parameters	HCM (n=20)	Controls (n=20)	P
Velocity (cm/s)	Mean ± SD	Mean ± SD	
IVSB S	4.71 ± 1.44	6.99 ± 1.33	0.0001
IVSB E	4.44 ± 2.46	10.17 ± 1.09	0.0001
IVSB A	3.69 ± 1.61	6.12 ± 1.96	0.005
E/A ratio	1.54 ± 1.39	1.87 ± 0.6	0.007
IVSM S	3.17 ± 1.35	4.53 ± 1.37	0.041
IVSM E	3.46 ± 2.13	8.69 ± 1.53	0.0001
IVSM A	3.03 ± 1.49	3.43 ± 1.79	0.849
E/A ratio	1.34 ± 1.15	3.37 ± 2.6	0.001
Strain rate (1/s)			
IVSB SR _S	1.95 ± 1.40	1.01 ± 2.40	0.330
IVSB SR _E	1.45 ± 0.07	1.68 ± 3.00	0.001
IVSB SR _A	1.15 ± 0.6	1.01 ± 1.80	0.001
IVSM SR _S	0.94 ± 0.63	1.79 ± 1.17	0.001
IVSM SR _E	1.15 ± 0.96	2.11 ± 1.11	0.006
IVSM SR _A	0.74 ± 0.46	1.12 ± 0.67	0.136
Strain (%)			
IVSB strain	17.58 ± 8.10	24.51 ± 7.80	0.034
IVSM strain	8.80 ± 4.60	23.53 ± 6.60	0.001
Velocity integral (cm)			
IVSB I	0.79 ± 0.30	0.79 ± 0.31	0.23
IVSM I	0.49 ± 0.23	0.74 ± 0.39	0.008

IVSB-S/-E/-A= interventricular septum basal segment velocity during systole S; and early E and late A diastole, IVSM-S/-E/-A= interventricular septum mid segment velocity during systole S; and early E and late A diastole, IVSBSR_E = interventricular septum basal strain rate E, IVSBSR_A= interventricular septum basal strain rate A, IVSMSR_E= interventricular septum mid strain rate E, IVSMSR_A= interventricular septum mid strain rate A, IVSB strain = interventricular septum basal strain, IVSM strain = interventricular mid segment strain, IVSBI= interventricular septum basal velocity integral, IVSMI= interventricular septum mid segment velocity integral.

3.4.3 Velocity and strain and strain rate in the right ventricular wall

The findings of the tissue Doppler imaging of the right ventricle revealed a significant reduction of the regional velocity at the base of the right ventricle free wall during systole, (S wave 8.38 ± 3.02 versus 10.05 ± 1.66 cm/s, $p < 0.05$) and insignificant changes during diastole (mean E wave

7.5 ± 3.64 cm/s versus 10.27 ± 3.38 cm/s, p = 0.06 and insignificant paradoxical A wave mean 7.62 ± 2.77 cm/s versus 6.64 ± 1.98 cm/s) (Fig. 14, Table 5). The RV velocity integral was reduced in HCM patients in comparison to the controls mainly at the mid segment (mean 0.64 ± 0.57 versus 1.45 ± 0.48 cm, p = 0.001). The regional strain rate value at the base of RV showed no reduction in the systolic phase. Similarly, SR_E showed a significant paradoxical change in HCM patients (mean 2.06 ± 1.6 1/s versus 2.51 ± 3.53 1/s, p = 0.001). SR_A was significantly reduced in HCM patients (mean 2.27 ± 1.88 versus 1.3 ± 2.93 1/s, p = 0.001).

At the mid point of the free RV wall a significant reduction of the velocity curve value was noted during systole (S wave) with mean of 4.46 ± 3.34 cm/s versus 8.37 ± 1.56 cm /s, p = 0.005 and E wave with mean of 4.02 ± 3.18 versus 9.82 ± 1.99 cm/s, p < 0.001. The velocity integral was more impaired at the mid segment (0.64 ± 0.5 cm versus 1.45 ± 0.48 cm, p = 0.001) than at the basal segment.

The mean peak systolic (SR_S) strain rate was significantly reduced (1.66 ± 1.04 versus 2.65 ± 2.3 1/s, p = 0.001), as was SR_E (1.45 ± 1.04 1/s versus 2.71 ± 1.5 1/s, p = 0.004) but no significant changes were found in the late diastole in comparison to the controls. The strain was significantly reduced at the mid segment in HCM patients (mean 17.4 ± 10.30 % versus 28.9 ± 10.4 % in controls, p = 0.01).

3.5 Regional atrial velocities and strain rates in HCM patients compared to controls

We observed a general slight impairment of the systolic and diastolic regional longitudinal velocities at the annular and mid segments of the LA, IAS and RA wall in HCM patients in comparison to the controls. A significant reduction of the regional velocities value in patients with HCM occurred at the annular of the interatrial septum during early filling; E wave was a mean of 4.01 ± 2.2 versus 8.77 ± 1.1, p = 0.001 and in mid segment IAS (3.23 ± 2.0 versus 6.01 ± 1.96, p = 0.001); there was no significant difference between the systolic velocities or diastolic velocities at other segments (Table 8). The pressure gradient across the LVOT is negatively correlated to early diastolic velocity (E) at the annular IAS (r = - 0.7, p= 0.01), to systolic velocity (S) at the RA annular segment (r = - 0.6, p= 0.02), and to late diastolic velocity (A) at the RA annular segment (r = - 0.5, p= 0.03).

Table 8: Comparison between the segmental delayed atrial velocity (cm/s) in HCM (n=20) and controls (n=20), (mean \pm SD)

Parameters	Velocity (mean SD)								
	S			E			A		
	HCM	controls	P	HCM	controls	P	HCM	controls	P
LA annular	5.03 \pm 2.2	6.70 \pm 1.6	0.07	5.74 \pm 3.0	8.69 \pm 3.9	0.1	3.77 \pm 1.3	5.14 \pm 2.4	0.2
LA middle	2.94 \pm 1.5	4.29 \pm 2.5	0.2	1.87 \pm 2.2	3.72 \pm 2.5	0.09	2.29 \pm 1.7	3.12 \pm 2.2	0.4
IAS annular	4.65 \pm 1.5	5.23 \pm 1.1	0.4	4.01 \pm 2.2	8.77 \pm 1.1	0.001	4.45 \pm 1.9	5.36 \pm 1.8	0.3
IAS middle	3.60 \pm 1.8	4.28 \pm 2.0	0.3	3.23 \pm 2.0	6.01 \pm 1.9	0.001	2.75 \pm 1.6	3.93 \pm 2.1	0.2
RA annular	6.17 \pm 2.9	7.59 \pm 2	0.2	4.96 \pm 3.4	5.79 \pm 2.8	0.3	5.87 \pm 2.7	5.30 \pm 2.9	0.6
RA middle	2.65 \pm 2.2	2.95 \pm 3	0.9	1.75 \pm 1.9	2.18 \pm 2.7	1.00	2.60 \pm 2.4	2.10 \pm 2.6	0.3

LA annular and middle: left atrial annular and mid segment, IAS annular and middle: interatrial annular and mid segment, RA annular and middle: right atrial annular and mid segment, S: systolic, E and A early and late diastolic velocities.

In control subjects and patients with HCM, we found that annulus segments had higher velocity than mid atrial segments (Figs. 19 and 20).

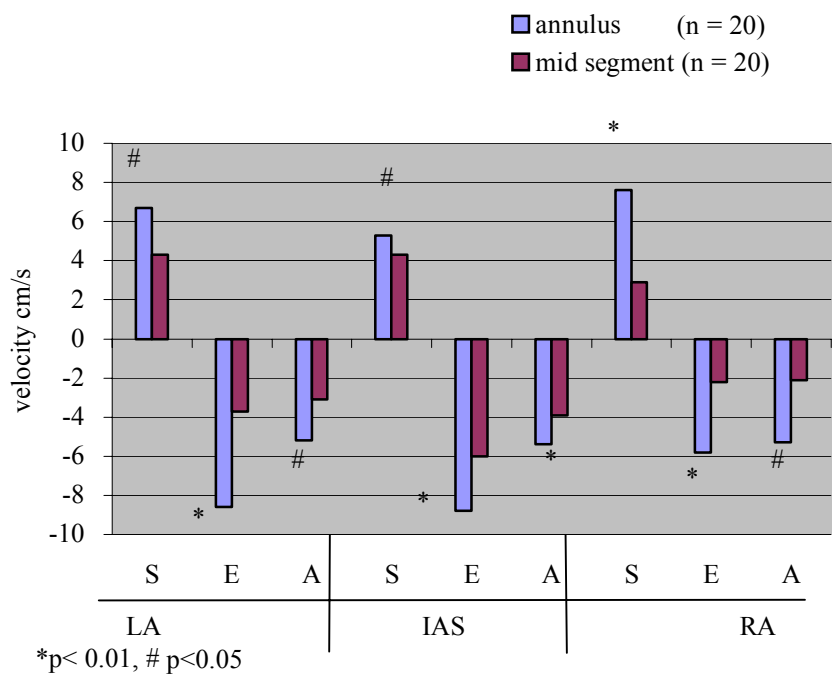


Figure 19: Difference in atrial velocities between annular and mid segments

Significant peak velocity differences between atrial annular and midsegments for each wall in controls LA: left atrial, IAS: interatrial septum, RA: right atrial, S: systolic, E and A: early and late diastolic peak velocities.

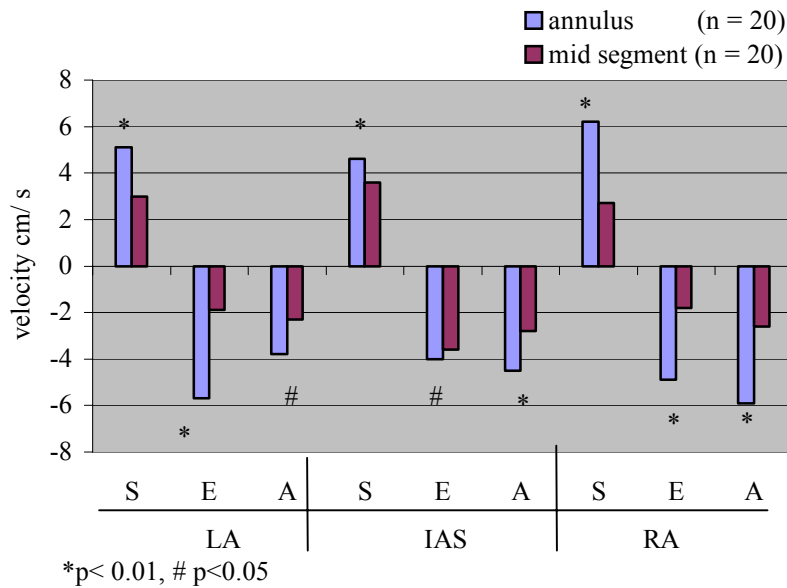


Figure 20: Distribution of atrial segmental velocity in patients with HCM.

Significant differences in peak velocity between atrial annulus and mid segments in patients with HCM. LA: left atrial, IAS: interatrial septum, RA: right atrial, S: systolic, E and A: early and late diastolic peak velocities

The strain rate in HCM patients was significantly reduced in the annular and mid segments of the LA lateral wall, IAS mid segment and right atrial annular segment in comparison to that in healthy subjects, as shown in details in (Table 9).

Table 9: Comparison between the atrial strain rate (1/S) in HCM (n = 20) and controls (n = 20) (mean ± SD)

Parameters	Strain rate 1/S (mean ± SD)								
	SR _S			SR _E			SR _A		
	HCM	controls	P	HCM	controls	P	HCM	controls	P
LA annular	1.59 ± 1.2	2.58 ± 0.8	< 0.01	1.77 ± 1.0	4.37 ± 1.9	< 0.01	1.26 ± 1.1	1.35 ± 0.7	0.3
LA middle	1.87 ± 0.9	3.71 ± 1.4	0.01	1.55 ± 1.2	4.46 ± 3.2	0.01	1.69 ± 1.7	2.94 ± 1.8	0.07
IAS annular	1.59 ± 0.9	2.38 ± 1.1	0.3	1.49 ± 1.1	2.38 ± 1.1	0.05	1.82 ± 0.8	1.91 ± 0.7	0.7
IAS middle	2.73 ± 1.5	4.60 ± 1.4	< 0.01	2.16 ± 1.3	5.39 ± 1.9	< 0.01	2.15 ± 1.1	3.54 ± 1.14	0.01
RA annular	3.67 ± 2.6	4.42 ± 1.4	0.3	3.67 ± 2.9	6.06 ± 2.6	0.02	3.99 ± 3.0	2.99 ± 2.0	0.4
RA middle	3.40 ± 2.1	4.25 ± 2.7	0.5	2.51 ± 1.9	3.71 ± 2.9	0.3	3.07 ± 2.1	3.11 ± 2.0	0.8

LA annular segment, IAS middle: interatrial midsegment, RA: right atrial, SR_S: systolic strain rate, SR_E/ SR_A: early and late diastolic strain rate. p < 0.05.

Patients with HCM had a significant reduction in the regional strain rates as follows: the annular left atrial systolic strain rate in HCM patients was 1.59 ± 1.21 1/s versus 2.58 ± 0.86 1/s, in controls, (p = 0.007), and mean diastolic early strain rate (SR_E) was 1.77 ± 1.02 1/s versus 4.37 ±

1.98 1/s, ($p = 0.001$). The systolic and diastolic strain rate is reduced at the septal mid segment: mean SR_S in HCM patients was 2.73 ± 1.55 1/s versus 4.6 ± 1.43 1/s, ($p = 0.007$), SR_E 2.16 ± 1.35 1/s versus 5.39 ± 1.93 1/s, ($p = 0.001$) and SR_A 2.15 ± 1.11 1/s versus 3.54 ± 1.14 1/s, ($p = 0.01$). The late RA annular Strain rate (SRA) is significantly reduced (3.67 ± 2.9 versus 6.06 ± 2.6 , $p = 0.02$).

In the IAS, the strain rate at the annulus is lower than at midsegment in controls, but inhomogeneous in HCM patients (Fig. 21 and 22).

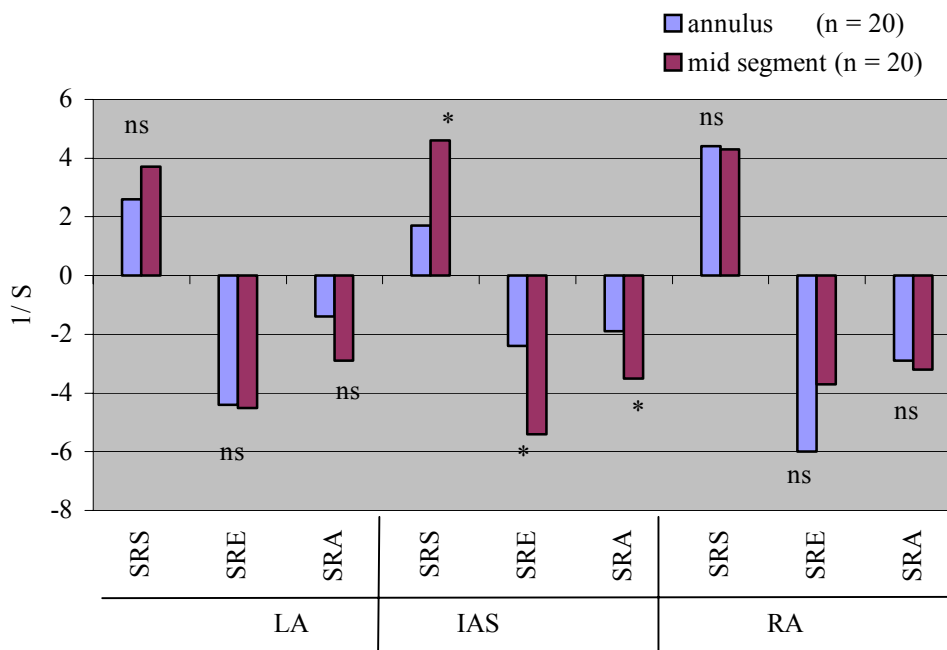


Figure 21: Distribution of strain rate in atrial wall segments in controls

SrS: peak systolic strain rate, SrE: peak early diastolic strain rate, SrA: peak late diastolic strain rate, Strain rate differences between annulus and mid segments in controls. LA: left atrial, IAS: interatrial septum, RA : right atrial.

Insignificant difference of strain rates between atrial annulus and mid segments of each wall in HCM patients

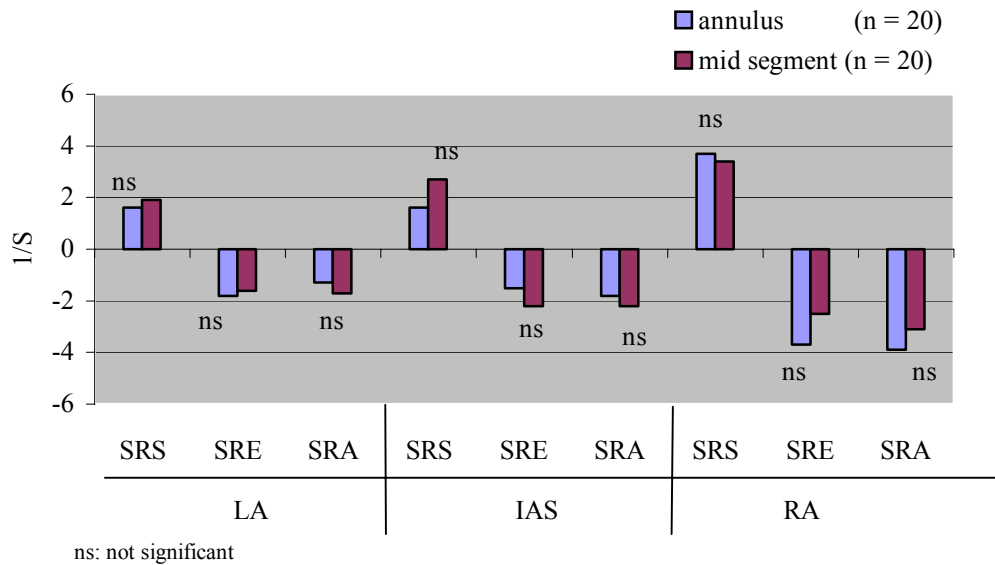


Figure 22: Distribution of strain rate in atrial wall segments in HCM.

Insignificant difference of strain rates between atrial annulus and mid segments of each wall in HCM patients. SRS: peak systolic strain rate, SRE: peak early diastolic strain rate, SRA: peak late diastolic strain rate, LA: left atrial, IAS: interatrial septum, RA : right atrial. NS : insignificant.

The LA lateral annular early peak strain rate is negatively correlated to the IVRT of the interventricular septum ($r = -0.6, p = 0.03$).

In patients with HCM, the pressure gradient load at the LVOT was negatively correlated to IAS annular peak SR_E ($r = -0.6, p = 0.02$), IAS mid SR_S ($r = -0.6, p = 0.03$), IAS mid SR_E ($r = -0.6, p = 0.04$), RA annular SR_S ($r = -0.6, p = 0.02$) and RA annular SR_A ($r = -0.5, p = 0.03$). Additionally, the LA lateral annular early peak strain rate is negatively correlated to the IVRT of the interventricular septum ($r = -0.7, p = 0.03$) which, is positively correlated to peak SR_S at the mid segment of the RA ($r = 0.6, p = 0.02$). This means that prolongation of IVRT decreases the regional early strain rate of the annular LA, and as a compensatory effect, increases the peak systolic strain rate at the mid segments of the RA when the IVRT is prolonged. Atrial velocities and SR were not associated with thickness of the IVS septum or heart rate.

3.6 Myocardial performance index and isovolumic intervals

A significant increase of myocardial performance index (mean 0.51 ± 0.11 versus 0.38 ± 0.07 , $p = 0.004$) and I/H index (mean 0.23 ± 0.06 versus 0.15 ± 0.03 , $p = 0.001$) were found in HCM patients in comparison to controls. The isovolumic relaxation and contraction period were prolonged in patients with HCM in comparison to controls (mean 84.1 ± 27.8 ms versus 60 ± 13.33 ms, $p = 0.004$) and IVCT was also delayed in patients with HCM in comparison to controls (mean 67.1 ± 17.13 ms versus 43.4 ± 8.6 ms, $p = 0.001$) Table10.

Table 10: Comparison of time intervals and indices between HCM to controls

Parameters	HCM (n = 20)	Controls (n = 20)	P
	Mean \pm SD	Mean \pm SD	
IVCT (ms)	67.13 ± 17.13	43.4 ± 8.60	0.001
ET (ms)	279 ± 32.26	270 ± 39.10	0.495
IVRT (ms)	84.1 ± 27.8	60 ± 13.30	0.004
Tei index	0.51 ± 0.11	0.38 ± 0.07	0.004
FT (ms)	419 ± 209	403 ± 80	0.683
I/H index	0.23 ± 0.06	0.15 ± 0.03	0.001

IVCT= isovolumic contraction time, ET= ejection time, IVRT= isovolumic relaxation time, Tei= Tei index, FT= filling time, I/H = isovolumic heterovolumic. ms; millisecond.

The ejection time and filling time revealed no significant differences between HCM and controls. The Tei index, which reflects global ventricular function, is not correlated to age in controls ($r = 0.1$, ns) or in patients with HCM ($r = 0.1$, ns). The Tei index in controls was associated with ET ($r = -0.7$, $p = 0.01$) and the I/H index ($r = 0.8$, $p = 0.001$), also in patients with HCM it was correlated to the I/H index ($r = 0.6$, $p = 0.02$) and to the IVRT ($r = 0.7$, $p = 0.001$) but it was not correlated to IVRT in controls. The Tei index was associated with LV lateral wall mid segment strain in HCM patients ($r = 0.6$, $p = 0.03$) but not in controls. The I/H index was correlated positively to IVS basal segment strain in patients with HCM ($r = 0.5$, $p = 0.02$) but not in controls.

4 Discussion

4.1 Hypertrophic cardiomyopathy: a rare heterogeneous myocardial disease

Vulpian first described hypertrophic cardiomyopathy in the year 1868 [35]. The German pathologists Schminke 1907 and Brock reported first intra-operative pressure measurements in patients with HCM [28, 36] and series of reports followed. In 1995 WHO/ISFG group agreed on the definition and the classification of cardiomyopathy according to its pathophysiology and pathogenesis (Table 11).

Table 11: The WHO classification of cardiomyopathy:

-
- Dilated cardiomyopathy
 - Hypertrophic cardiomyopathy
 - Restrictive cardiomyopathy
 - Rhythmogenic right ventricular cardiomyopathy
 - Unclassified cardiomyopathy
 - Specific cardiomyopathy:
 - Ischemic
 - Valvular
 - Hypertensive
 - Inflammatory
 - Metabolic
 - Systemic diseases
 - Muscular disease
 - Neuromuscular diseases
 - Allergic toxic
 - Peripartum
-

Hypertrophic cardiomyopathy (HCM) is a rare heterogeneous disease affecting cardiac muscle with a wide spectrum of manifestations. Left ventricular outlet tract (LVOT) obstruction is present in 20 to 30 % patients with HCM [37]. In western populations the prevalence is estimated at 1:500 [38]; recently, the incidence of HCM has been 1: 500 in the general population and it remains the most common cause of sudden death in children and young adults before the age 35 [9]. HCM has been described in infants and young children but data on the manifestation and ventricular function in children are limited. Children diagnosed before 14 years of age have been found to have a worse prognosis when they reach adolescence and early adulthood with an annual incidence of sudden death of 2-4% [39]. Adults are often asymptomatic but their estimated mortality may be as high as 1-2% per annum [39-42]. The

major risk of HCM is sudden cardiac death, which may occur even in asymptomatic patients without hemodynamic obstruction [43]. Arrhythmia, hypotension, altered autonomic function including vascular control and ischemia are likely to act as triggers for sudden death [44]. Risk factors for sudden death in HCM are listed in Table 12 [8, 45, 46].

Table 12: The Factors that increase the risk of sudden death in patients with hypertrophic cardiomyopathy

- Identification of a high-risk mutant gene
- Family history of HCM related sudden death
- Pre-syncope or reanimation situation
- Persistent supraventricular tachycardia
- Ventricular tachycardia
- Abnormal blood pressure response to exercise
- Marked ventricular hypertrophy is controversial

The molecular genetics, pathogenesis, familial types and treatment of hypertrophic cardiomyopathy have been fully discussed in many published articles [5, 43, 47-54]. Molecular genetic studies over the past decade have underscored and provided important insights into the profound clinical and genetic heterogeneity of HCM, including the power to achieve preclinical diagnosis of individuals who are affected by a mutant gene but who show no evidence of the disease phenotype on a two-dimensional echocardiogram or electrocardiogram [6, 46, 55, 56].

The complete diagnosis can only be reliable when all the implicated gene loci have been identified. Laboratory DNA analysis for mutant genes is the most definitive method for establishing the diagnosis of HCM. At present, however, there are several obstacles to the translation of genetic research into practical clinical applications and routine clinical strategy. These include the substantial genetic heterogeneity, the low frequency with which each causal mutation occurs in the general HCM population, and the important methodological difficulties associated with identifying a single disease-causing mutation among 10 different genes in view of the complex, time-consuming, and expensive laboratory techniques involved.

Until then the combination of electrocardiogram and echocardiography, in conjunction with other clinical information, remains the most useful for the diagnosis of patients with HCM [44].

4.2 Hypertrophic cardiomyopathy

4.2.1 Clinical presentation

Clinical presentation (symptoms and the clinical findings in different forms of HCM) have been studied and published in several articles [57-59]. The clinical manifestations in our patients are shown in Figures 12 and 13 which show the early onset of HCM in our pediatric patients (65% before entering school and 95% before reaching the age of 13).

The LV hypertrophy progression is frequent among children and adolescents, but is absent in adults [60], and it has long been recognised that left ventricular hypertrophy is relatively unusual in childhood, but typically develops during the pubertal growth spurt [61]. The early finding of heart murmur on simple auscultation in a child with positive family history of heart disease is very indicative. About 60% of our patients were referred for further cardiac evaluation due to a 2-3/ 6 systolic murmur in the precordial area; 25% of the studied patients were diagnosed by echocardiography during screening of family members of one person diagnosed with HCM. Moreover, in our series of patients asymptomatic presentation of HCM was found in 80% of the cases. Children with heart murmur and positive family history of HCM whose echocardiographic examination does not confirm HCM should be monitored. Exertional dyspnoea and cyanosis or syncopal attack, and failure to thrive are clearly other aspects of the wide (heterogeneous) picture of the clinical presentation of this disease in our cases Fig.13. The associated defects like VSD and other cardiac anomalies may complicate the therapy of the HCM patients. An unusual association of HCM with complete AV-canal and trisomy 21 was reported by Eidem BW in a single case [62]. In our cases, about the half of the cases have the SAM phenomena, which seems to be a component feature of the hypertrophic changes in the interventricular septum, but this is not specific for HCM and has been demonstrated in other conditions, including hypertensive heart disease [61].

4.2.2 Hypertrophic cardiomyopathy: Treatment

The fact that most of studied cases (50%) were initially diagnosed in the preschool age of ≤ 6 years indicates that the rapid changes in the hemodynamic state of HCM patients occur with normal somatic growth [63]. The short interval between the initial diagnosis of the disease and the indication for intervention (median 5.9 years, range 1 month to 12 years) indicates the rapid development and the progressive nature of the disease, despite medical treatment, whereas 90% of our cases received medical treatment with beta-blockers or verapamil. While in only half of the cases (55%) surgical intervention (septal myectomy) was indicated, the other half (45%) are

doing well under medical therapy; echocardiographic examination showed no severe progressive obstruction and the patients are less symptomatic. Administration of verapamil has been found to improve global LV filling and clinical manifestations, and beta-blockers seem to improve survival in childhood HCM [64, 65]. Disopyramide is valuable in relieving the symptoms of patients with HOCM before surgical septal myectomy [66]. Patients with hypertrophic cardiomyopathy can have varied pathophysiological courses, and may have heterogeneous clinical manifestation, which require different therapeutic modalities. Treatment modalities include symptomatic treatment, general activity restriction, drugs, dual chamber pacing (pacemaker/defibrillator implantation), cardiac catheter intervention (percutaneous alcohol septal ablation) and operative approaches (myectomy) in failure of medical treatment [45]. The goal of therapy or intervention is to relieve the symptoms and improve life quality of the patients; patients who are genetically affected with or without HCM phenotype (LVH) require longitudinal follow up with specific treatment for the symptoms. Those adults with high risk for sudden death (Table 12) are managed with primary or secondary prevention of sudden death by implantation of intracardiac defibrillator. Patients with mild or no symptoms (low sudden death risk) are managed without drugs or with beta-blockers/verapamil as needed. The patients with progressive heart failure symptoms are treated with beta-blockers, verapamil or disopyramide. Those, who developed atrial fibrillation (25% of HCM with paroxysmal episodes/or chronic) are treated with anticoagulants, antiarrhythmics and cardioversion or pulmonary vein ablation/MAZE procedure, and pharmacological rate-control procedure. The patients who developed drug refractory symptoms due to obstructive HCM either at rest or under provocation are treated with surgical septal myectomy (gold standard) procedure or alternatives to surgery like septal ablation (if there is no associated cardiac structure or coronary abnormalities and surgery is contraindicated or rejected) and dual-chamber (DDD) pacing.

In children, depending on the severity of left ventricular outflow obstruction and LV-function, treated with medication and followed up, the gold standard therapy was septal myectomy. Pacing therapy has no role in the management of HCM in children. Randomized clinical trials that have been performed regarding pacing therapy have not shown a significant benefit. In addition, there has been no other data to contradict these findings [9].

While HCM has been considered a clinical implication for implantable cardiac defibrillator placement in children, careful patient selection is advised. Because of the high frequency of complications, including death at implantation, this therapy should be considered for patients for secondary prevention after an episode of resuscitated sudden death or for primary prevention for those patients with multiple risk factors.

Septal ablation is not applicable in children, because small children have relatively small coronary arteries and high incidence of recurrence of revascularization and septal hypertrophy. One of our patients required 3 times repeated alcohol septal ablation because of recurrent obstruction 1-3 months after the procedure. One of the major concerns regarding alcohol septal ablation relevant to the child or young adult with symptomatic obstructive HCM is the potential long-term risk for arrhythmia-related cardiac events, including sudden cardiac death, arising from the procedure itself. The risk of such an event may well outweigh the risk of sudden cardiac death from the disease itself and, for this and other reasons, there is no role for alcohol ablation in the treatment of children and adolescents [67].

HCM patients with non-obstructive type who have refractory drug symptoms require ultimately heart transplant at end stage after failure of the therapy with diuretics, beta-blockers, digoxin, and spiro lactone. Emergence of new experiences in adults in favour of the septal ablation more than surgery gives further aspects to the strategy of HCM therapy. Subgroups of HCM need surgical septal myectomy, particularly, those with associated cardiac structure abnormality like severe mitral regurgitation or intrinsic mitral valve diseases, VSD, fixed subaortic stenosis and coronary artery diseases requiring coronary By pass operation in adults.

Nevertheless, some of the available, nonrandomized comparative analyses suggest that gradient reduction by alcohol septal atrophy (ASA) is somewhat less consistent and complete than with surgical myectomy [68, 69]. Since the long-term safety of ASA remains to be established, the current American College of Cardiology/European Society of Cardiology (ACC/ESC) guidelines support the view that surgical septal myectomy should represent the gold standard treatment for drug-refractory patients with obstructive HCM, particularly in the young, while ASA should be considered an important complementary treatment option to be preferred in those patients who are elderly, have increased operative risk, do not have access to expert surgical centers, or reject operation [8].

In patients with midventricular obstruction, the risk of recurrence may be even higher than in the classic form of outflow obstruction [70]. Therefore, surgery should be considered the first choice in these patients.

Although there is interest in the application of gene therapy to a variety of inheritable human conditions, at this time the clinical utilization of this technology in HCM is problematic. Hypertrophic cardiomyopathy is transmitted as an autosomal dominant trait, and affected persons possess one mutated and one normal allele. Because most mutations in this disease cause substitution of a single amino acid within the encoded protein, gene therapy would theoretically have the difficult task of selectively targeting and inactivating the mutated gene, the encoded

protein, or both. Furthermore, selection of patients for gene therapy would be particularly complex given that some forms of the disease are compatible with normal longevity and absence of symptoms. Also, such therapeutic interventions would presumably be applicable only to a small patient subset consisting of very young affected members from high-risk families identified prior to the development of LVH. Recent study revealed the association of certain gene mutation with moderately increased risk of sudden death in HOCM patients [46]. Genetic analysis ultimately may help to identify patients at high risk for complications such as ventricular arrhythmia and ventricular tachycardia in familiar HCM without LVOTO, who will require a particular treatment strategy such as the implantation of a defibrillator [46, 71-75].

4.3 Tissue Doppler echocardiography (TDE) and heart function

4.3.1 Limitations of conventional echocardiography in quantification of myocardial regional function

Conventional echocardiography and ECG are simple methods to diagnose hypertrophic cardiomyopathy. However, most of the currently available echocardiographic techniques are not able to offer precise quantification of regional myocardial contractile function. Echocardiographic evaluation of global left ventricular function is most commonly obtained by visual semi-quantitative analysis. Measurements of fractional shortening (FS), stroke volume and left ventricular ejection fraction (LVEF) are frequently assessed parameters and are normal in most of the patients with HCM. However, in many patients accurate estimation is limited by poor image quality and variation of ventricular wall thickness [76], and by paradoxical movement of the IVS. In the obstructive forms of HCM, the complexity of pathophysiological interaction makes conventional echocardiographic functional assessment extremely difficult and complex [77]. Furthermore, the assessment of diastolic function by conventional echocardiography relies on the study of mitral inflow velocity profile, but this is of limited value in the presence of atrial fibrillation or other arrhythmia. Non-invasive tissue Doppler imaging has enabled the clinician to explore the longitudinal regional velocity changes of the myocardium in patients with myocardial diseases and to determine the global and regional myocardial function.

Previous studies have validated the accuracy and reproducibility of velocity measures by TDI with in vitro models and in humans [20, 78, 79]. The myocardial velocity gradient (MVG) and the strain measured in early diastole would appear to be an accurate variable used to discriminate

between HCM and hypertrophy in athletes [80]. Shimizu reported that the diastolic function of LV could be non-invasively assessed by TDI at annular basal segments of the mitral valve [81]. Doppler tissue imaging (DTI) allows the measurement of longitudinal and radial myocardial velocities throughout the cardiac cycle, as well as the time intervals, with a high precision.

4.4 Tissue Doppler imaging and cardiac function assessment: LV systolic function

4.4.1 Qualitatively assessed velocity curves: normal and HCM pattern

The normal pattern of the tissue Doppler velocity curve obtained in four chamber view is shown in Figure 3a. The wave S, E, and A represents the systolic and early and late diastolic movement, respectively. The normal velocity of the myocardial muscle is characterised by normal basal apical velocity gradient. In HCM patients the velocity is reduced and the peaks of the S, E and A wave are reduced. The S wave reaches its peak later than in the controls, with the same basal apical velocity gradient (Fig. 3b).

4.4.2 Regional left ventricular longitudinal systolic function and velocity profiles

Tissue Doppler echocardiography (TDE) is an evolving non-invasive tool complementing conventional echocardiography in the assessment of left ventricular systolic and diastolic function in various clinical conditions. Echocardiographic evaluation of global left ventricular function is most commonly obtained by visual semi-quantitative analysis. Measurements of fractional shortening (FS), stroke volume and left ventricular ejection fraction (LVEF) are frequently used as mentioned above. However, in many patients accurate estimation is limited by poor image quality. In our study conventional echocardiographic examination revealed non-compromised LV systolic function with FS of mean 45 ± 13 %) and mean EF of 73 ± 18 %. This finding may be affected by mitral insufficiency, which was found in 65% of our cases. Less dependent on endocardial definition in conventional echocardiographic examination, TDI has been evaluated in different patient groups for assessment of the LVEF. Measurement of longitudinal shortening of the left ventricle to assess LV function has gained growing importance during the last years [76]. Left ventricular long axis contraction is reflected in mitral annular descent, which can be evaluated by TDI at different sites. In comparison with radionuclide ventriculography the septal and lateral average velocities were well correlated with LVEF under identical conditions, and this relationship was not significantly affected by wall motion abnormalities [82]. In our study the peak myocardial velocities at basal and mid segments of the LV free wall and IVS are significantly reduced in systole, which indicates the reduction of the

regional left ventricular longitudinal systolic shortening in the patient group in comparison to our controls. In consistent with the findings of Gulati who found that a peak mitral annular descent velocity of > 5.4 cm/s identified LVEF within normal range with reasonable sensitivity and specificity [82].

In contrast to Yamada et al. who found a significant positive correlation of endocardial peak systolic velocity for the LV posterior wall with FS and LVEF in different patient groups but no correlation between FS or LVEF and peak velocity of the ventricular septum [83], we did not find any significant correlation between peak systolic longitudinal velocity and FS or EF. This may be explained by the contractile longitudinal movements of the IVS in contrast to the LV lateral wall. In addition, no association was found to the thickness of IVS or gradient at the LVOT.

The distribution of the longitudinal velocities profile in the LV free wall and IVS in our patient group was inhomogeneous with basal to apical gradient; also we found the same pattern of velocity gradient profiles in the controls, similar to findings reported in many previous studies [84, 85]. Additionally, we observed a significant difference between the lateral wall and IVS velocities, consistent with those who reported that the lateral walls are less affected than the septum [86-88].

The time (in ms) taken by the longitudinal velocity S wave to reach its peak is delayed in HCM patients in comparison to the controls (Fig 17), which is due to the impaired relaxation of the myocardial myofibrils. An increase in fibrotic tissue was found in myocardial autopsies from patients with HCM [89-91]. These results revealed an impairment of the regional longitudinal systolic function of the LV in patients with HCM.

4.5 Regional LV longitudinal systolic function: strain rate and strain curves

4.5.1 Tissue Doppler patterns of strain rate: normal and in HCM patients

As has been mentioned in the velocity curve the strain rate of the ventricles obtained in four chamber view demonstrated the strain rate curves, which are represented by a negative (SR_S) and positive (SR_E) and (SR_A) waves for the systolic and diastolic phases. The directions of the strain rate waves are opposite to those of the velocity curve. The SR_S wave represents the strain rate (deformation) during the systolic time of the cardiac cycle, the SR_E wave represents the early

diastolic filling wave and SR_A the late diastolic filling (Fig. 5). The normal longitudinal strain rate is homogeneous in the heart segments.

In HCM, strain rate pattern shows that the value of the corresponding waves is reduced in comparison to those of the controls (Fig. 5b) with loss of the homogeneity and occurrence of paradoxical strain rate.

4.5.2 Tissue Doppler patterns of strain: normal and in HCM patients

The deformation curve (strain) shows a symmetrical pattern with one peak during the systolic phase and shortening of the myocardial muscle and it is homogenous in heart segments (Fig.6). Strain in basal and mid segments of the lateral walls as well as of the interventricular septum were always negative representing shortening of myocardial fibers during systole and showed parallel changes in healthy individuals. In patients with HCM the strain curve shows the reduced regional shortening of the myocardium at different segments mainly in the interventricular septum (Fig. 7).

4.6 Longitudinal ventricular regional strain rate and strain profiles

In the last years increasing numbers of clinical studies have indicated that the TDI strain rate and strain are feasible and non-invasive tools to evaluate the systolic and diastolic function of the heart. Urheim S. et al stated that Doppler derived strain rate and strain reflect more directly the assessment of regional function than tissue velocities, which are influenced by contractile function of other myocardial regions and the overall movements of the heart due to tethering effects [14]. Similarly, Greenberg reported that strain rate and strain are more accurate than tissue velocities indices for assessment of the myocardial contractility [92]. In our study the regional longitudinal strain rate of the LV free wall at basal and mid segments is significantly altered during systole in patients with HCM. However, at LV mid wall, the mean systolic strain rate value is paradoxically reversed (1.52 versus 1.23, $p = 0.001$), which also is below the normal value reported by Weidemann et al [93]. Reduced SR in the early filling phase at the basal and mid septal segment indicates the impairment of myocardial relaxation due to this myopathic process involving mainly the IVS and the heterogeneity of SR distribution in heart segments may explained by the segmental structural changes and myocardial disarray which is a main feature of HCM pathology.

The systolic strain rate showed a significant reduction in patients with HCM at the middle of the septal wall, and paradoxical strain rate at the LV mid segment; this may be a compensatory action (interaction) for the reduced mid septal wall strain rate.

The longitudinal regional strain of the IVS at the mid septal segment is significantly reduced in our group of patients with HCM ($p = 0.001$) and at the basal septal segment ($p = 0.03$). There was a moderate relationship ($r = 0.6$, $p = 0.03$) between the regional strain of the LV free wall at mid segment and global ventricular function evaluated according to the myocardial performance index (Tei index) in patients with HCM. Similarly, a positive relationship ($r = 0.6$, $p = 0.02$) was found between the IVS basal strain and the isovolumic/heterovolumic index (I/H index). This may indicate a significant reduction of the regional strain due to compensatory action for the reduced myocardial performance or because of segmental structural changes of the myocardium. Further detailed studies might explore these changes. There was no association between the strain and the intracavitary obstruction or loading LVOT gradient, or between the interventricular septum thickness and strain.

This finding of impairment of the regional systolic function of the LV, as has been reported in some studies, is consistent with Urheim [14] findings. They reported that myocardial strain is a powerful tool for quantifying regional myocardial function independent of load condition [14], and that strain is less influenced by tethering effect than the myocardial velocity.

From the tissue Doppler findings we infer that the regional longitudinal systolic function of the left ventricle is significantly reduced as represented by the low systolic velocities profiles at all examined heart segments and reduction of the systolic strain rate or paradoxical strain rate and strain at the mid segment of the lateral LV and septal walls. The myocardial deformation which may represent the contractile function more accurately is dramatically reduced in the septal wall at the basal and mid segments respectively. The heterogeneity of regional function (strain/strain rate) in these patients may reflect the regional variation in the myocardial disarray and fibrosis that is characteristic of this disorder.

Although the global systolic function of the heart is normal or increased in patients with HCM as has been documented by conventional echocardiography (EF) in our patients and other reports, the tissue Doppler technique revealed new insights into the inhomogeneous alterations of the longitudinal regional myocardial function estimated by strain/strain rate imaging.

4.7 Regional longitudinal diastolic dysfunction of LV

By quantifying changes in myocardial velocity throughout the cardiac cycle, TDI is also beneficial in the assessment of diastolic function [20]. Our study demonstrates the general impairment in the diastolic regional longitudinal velocity of the LV free wall and IVS in patients with HCM in comparison to controls (Table 5). In addition, the diastolic wall velocities in HCM

were also reduced in comparison to the normal values for the corresponding E and A waves at respective segments published by Weidemann [93]. Also the E/A ratio at different myocardial segments, mainly in the basal ($p = 0.007$) and mid septum ($p = <0.001$) segment, is significantly reduced in HCM patients in comparison to the controls. The other examined segments showed insignificant changes.

Stoylen and co-workers compared the strain rate in normal individual and reduced diastolic function and found that peak strain rate can describe the two mean diastolic events early and late filling. Strain rate is reduced in early filling in patients with reduced diastolic function and these findings are consistent with those shown by pulsed DTI at the mitral annulus [16].

The longitudinal regional diastolic strain rate, as demonstrated in normal subjects by Weidemann and Sun, is homogenous in the 4-chamber echocardiographic apical view of IVS segments [93]. Our study demonstrates the loss of this homogenous distribution in HCM patients whereas the E strain rate is mainly reduced at the basal septal segment. The regional longitudinal diastolic function of the left ventricle is impaired in patients with hypertrophic cardiomyopathy and it is mainly represented by the reduction of the regional longitudinal diastolic strain rate value as compared to that of the controls.

In accordance with our results we emphasize that tissue Doppler strain rate imaging is useful and complementary to standard Doppler imaging to characterize abnormal diastolic properties in HCM, reflecting a typical pattern of intramyocardial impaired relaxation at the level of hypertrophied septum.

4.7.1 Characteristics of the velocity curves in the interventricular septum: qualitative TDI

In the 2-D imaging, differentiation between the LV and RV part of the septum is possible. In addition, different patterns of contractile function were found in the RV and LV part of the IVS in a longitudinal manner.

Qualitatively, the velocity curves in septal wall revealed a mid to basal gradient in HCM patients as well as in controls, but an interesting finding is a difference in the velocity between the two sides of the septum: the right side has faster velocity than the left side of the IVS septum. In addition, the strain shows higher values in the right side of the septum than in the left side in HCM patients; such differing patterns in regional contractile function were not found in normal hearts. The velocity integral, however, shows no difference between HCM patients and normal controls. This heterogeneity of distribution in longitudinal regional myocardial velocities within the right and left ventricle may be explained by the differing regional myocardial fibre

architecture. Longitudinal or oblique fibres dominate within the right free wall, whereas circular mid-wall fibres are dominant in the left ventricular lateral wall and there is a mixture of both types within the ventricular septum [94].

4.8 RV function in hypertrophic cardiomyopathy and tissue Doppler imaging

Despite the importance of assessing RV function in many paediatric cardiac conditions, evaluation of RV function by echocardiography remains difficult due to the complex geometry of this chamber. Unlike the left ventricle (LV), the RV has no axis of symmetry, complicating the task of geometric modelling. Due to this geometric complexity, methods that traditionally have been used to assess LV function, such as ejection fraction (EF) and fractional shortening, are of limited value for assessment of RV function. Additionally, delineation of RV endocardium by echo is difficult due to the prominent endocardial trabeculations of the RV, and its retrosternal location, which limits acoustic access. Due to the complex morphology of the RV, tissue Doppler methods represent an attractive alternative for assessing RV function, as they do not depend upon accurate anatomic measurements. Recently, the novel TDI procedure has been used to evaluate RV function; Dagdeviren reported that the analysis of tricuspid annular velocities obtained by tissue Doppler technique is a practical method of the assessment of right ventricular systolic function [95]. In a clinical study, Efthimiadis and co-workers found that patients with HCM compared with controls had significantly lower right ventricular E/A ratio, and prolonged RV-IVRT which significantly correlated with that of the left ventricle [96]. An important finding of our study is that patients with hypertrophic cardiomyopathy, although asymptomatic, had evidence of right ventricular systolic and diastolic dysfunction; which is in consistent with the above findings. The RV free wall peak systolic and diastolic velocities, strain rate values and strain at basal and mid segment are significantly reduced in patients with HCM in comparison to controls and this may be a compensatory action due to reduction of LV regional function due to interventricular reaction or more probably due to segmental structural changes of the RV because of hypertrophic myocardial disarray.

The Tei index evaluates global ventricular function by measuring the ratio of isovolumic time intervals to ventricular ejection [23]. Conventionally, these intervals are measured from Doppler flow signals. Earlier studies found the Tei index to be useful in evaluating RV function in patients with CHD [97].

TDI-derived Tei index was employed to evaluate RV function [98, 99]. Our study revealed an impairment of RV function as observed with TDI-derived Tei index. In experimental studies

strain and strain rate imaging as load-independent parameters, have been validated and confirmed as evaluating RV contractility [30]. The significant alteration of strain and strain rate of RV, indicating impaired contractility of the RV in our patients with HCM in comparison to the control group. Our study confirmed the reduction of regional longitudinal right ventricular function in patients with HCM.

This heterogeneous distribution in longitudinal regional myocardial velocities within the right and left ventricle may be explained by the differing regional myocardial fiber architecture, as has been discussed for the IVS. Although the clinical significance of this finding is unclear at this time, it may indicate that patients with HCM have subclinical impairment of right ventricular diastolic function. Other authors have also documented comparable results [96].

4.9 Ventricular interaction

The forces that are transmitted from one ventricle to the other ventricle through the myocardium or pericardium, independent of neural, humoral or circulatory effects are interdependent. This is a result of close anatomic association between the ventricles; they are encircled by common muscle fibres, share a septal wall, and are enclosed within the pericardium. Diastolic and systolic ventricular interaction has been reported in many experimental and clinical studies [100-113].

Right ventricular (RV) function is often involved in left ventricular (LV) pathologies as a consequence of a direct injury extension, afterload changes or ventricular interdependence, which is mainly due to the close anatomical association between the two ventricles. In physiological or pathological conditions the volume or pressure overload of one ventricle leads to changes in the other ventricle. The right ventricular systolic pressure may result from the left ventricular contraction in 20 to 40 % and about 4% to 10% of the left ventricular systolic pressure may result from right ventricular contraction [105].

Increasing RV volume causes not only septal deviation but regional deformation in the left ventricular free wall as in an atrial septal defect [114].

The findings of these studies imply that ventricular interdependence causes overall ventricular deformation. Furthermore, Slinker et al ([115] reported that direct interaction was less important in hearts with concentric hypertrophy than in normal hearts because the septum was thicker and, hence, less distensible. RV relaxation is influenced by direct anatomic ventricular interaction [116] and RV function is affected by the impairment of LV function [117]. Ventricular interaction occurs directly and through the septum. As has been reported, in HCM patients the

reduction of regional diastolic function in non-hypertrophied RV is related to septal parameters [118].

In our study, by tissue Doppler technique, we confirmed alteration of the regional RV function in HCM patients in comparison to controls. Our findings confirm the reduction of systolic and diastolic regional RV function in HCM. Moreover, the RV regional strain is positively related to regional strain of IVS; a decrease in the regional deformation of the hypertrophied IVS leads to a decrease in the RV regional contraction and a decrease in the regional deformation of the LV. The impairment of the regional RV function in our patients with HCM might be explained on the grounds of a direct involvement of RV wall by myopathic process, since the HCM is a genetic disorder where the mutations are generally expressed in both ventricles. On the other hand, the altered RV function found in HCM patients in comparison to controls suggests that ventricular interaction may be an alternative explanation for the altered RV function detected by strain/strain rate imaging.

4.10 Myocardial strain and strain rate measurement: A non-invasive method for quantifying regional myocardial function

Strain and strain rate can detect the early impairment of longitudinal systolic function at the time when fractional shortening remains normal [119]. Tissue Doppler-derived strain and strain rate are more direct measures of regional function than tissue velocities, which are also influenced by contractile function of other myocardial regions due to tethering, and as load-independent parameters have been validated in experimental studies and confirmed as evaluating myocardial contractility [14, 30].

Experimental clinical studies carried out by many authors revealed that strain and strain rate imaging are valuable technique for quantifying regional myocardial deformation, contractility and differentiation between normal and diseased myocardium [13, 14, 17, 18, 92, 93, 120]. Strain and strain rate measurement are superior to two-dimensional dobutamine stress echocardiography (DSE) and tissue Doppler imaging for the assessment of myocardial viability [121].

Hua found that mid septal strain was significantly reduced in patients with HCM [122], strain has potential clinical applications to compensate the shortcomings of velocity and to be added to the routine echocardiographic procedures to make possible more accurate assessment of regional myocardial dysfunction. Similarly, systolic myocardial SRs were lower in hypertrophic cardiomyopathy patients than in athletes, hypertensive patients, and healthy subjects. Early

diastolic SR_E was able to discriminate between hypertrophic cardiomyopathy and physiologic hypertrophy in athletes [80].

In healthy subjects with 4-chamber view TDE the longitudinal strain rate/strain is homogeneous throughout the septum and LV walls. This is in contrast to the normal base-apex velocity.

In our patients with HCM strain rate and strain are reduced mainly in IVS segments in comparison to controls.

4.11 Global myocardial function: myocardial performance index (Tei index)

Quantitative recording of systolic and diastolic velocities can be done by TDE, which can precisely differentiate phases of the cardiac cycle. The Tei index measures the ratio of total time spent in isovolumic activity (isovolumic contraction time and isovolumic relaxation time) to the ejection time. Benjamin and co-workers reported that the Tei index offers easily-obtained, quantitative, reproducible assessment of right and left ventricular function. Increasing values of the myocardial performance index correlated with increasing degrees of both right and left ventricular dysfunction in a model of congenital heart disease with distorted ventricular morphology [123]. These observations suggest that the Tei index is useful as a means of quantitating ventricular function in these patients.

4.12 Doppler derived Tei index as a global parameters of left ventricular systolic and diastolic function

The recently proposed Doppler derived myocardial performance index (Tei index), which combines systolic and diastolic time intervals, has been reported to be a simple and reproducible index for assessing left ventricular function. However, assessment of right ventricle function using the Tei index is limited due to variation in isovolumic relaxation and contraction times, which are significantly influenced by respiration. These time intervals have been shown to be independent of blood pressure and ventricular geometry [23, 24, 124, 125]. LaCorte used a porcine model to directly correlate the Tei index with invasive indices of systolic and diastolic function and found a direct correlation between the Tei index and the systolic and diastolic invasive measurement and suggested clinical use of Tei index for assessment of global ventricular function [126].

Non-invasive echocardiographic indices of ventricular function are of great clinical importance in diagnosing and managing heart disease. The Tei index is easily obtainable and has been

clinically useful in assessing global ventricular function in fetuses [127, 128], children [97, 123, 129, 130] and adults, in various heart diseases [24, 25, 124, 125, 131-134].

Tarkan demonstrated that Tei index can be measured by tissue Doppler and that it correlated well with conventional Doppler derived Tei index. Moreover, tissue Doppler derived Tei index has the advantage of assessing both regional and global myocardial performance, and also has the ability to record systolic and diastolic velocity patterns simultaneously [33, 135, 136].

4.13 Atrial function

The atria serve as reservoirs and conduits for the passage of blood from the pulmonary veins to the left ventricle and from the superior and inferior caval vein to the right ventricle and as contractile chambers that augment left ventricular filling [137, 138]. Previous studies indicate that the atria contribute up to 30% of left ventricular filling and cardiac output and are particularly important in the setting of impaired left ventricular function.

To our knowledge, comprehensive segmental contraction of the body of the atria has not been studied and atrial functions in patients with HCM have not been evaluated.

Earlier work has examined differences between contraction velocity of the left atrial appendage and body [139] and differences in blood flow velocities within the atrium [140]. The atrial wall motion is complex, containing as it does both active and passive components of wall motion, and is also markedly influenced by overall heart motion. It is different for each atrium and varies with atrial size, loading conditions, atrial rhythm and atrial contractility and compliance. The velocity profiles for longitudinal regional atrial motion can be recorded from the walls of both atria using colour Doppler myocardial imaging. The best recordings of atrial motion are usually obtained from apical scanning.

4.13.1 Longitudinal atrial segmental velocity profiles

The atrial velocity curve is characterized by the three main waves S, E, A, which coincided with the ventricular systolic, early diastolic and late diastolic periods respectively (Fig. 12a). The normal pattern of atrial longitudinal regional velocities is characterized by the finding that the annular segments of the atrial walls and interatrial septum have higher velocities than the corresponding segments at the level of mid segments (Fig. 19). The additive translation from cardiac motion may contribute to increased velocities in the atrial segment adjacent to the annulus. The superior segments are stationary and do not contribute to the atrial motion, there is

an inhomogeneous velocity distribution between the different segments and between the lateral atria walls and interatrial septum consistent with findings by Thomas L [34].

In HCM patients, the lateral left and right atrial walls revealed no changes of the regional velocities (S, E or A) when compared to controls. The only remarkable velocity changes we have noted are that of peak early wave (E) of the interatrial septum at the annular and mid segment of the septal wall in patients with HCM in comparison to healthy subjects (Table 8). Because the atrial walls contribute no motion during the early diastolic ventricular phase, reduction of the E velocity in IAS may reflect delayed relaxation of the ventricular septum as shown by the prolongation of IVRT of the interventricular septum. The A velocity, which correlated to atrial pump, was not reduced in patients with HCM. In addition, the changes in regional velocities may not reflect the real contractility of the myocardium because the local velocity of a specific atrial region does not differentiate between active contraction and passive motion related to cardiac translation [34].

4.13.2 Pattern of atrial strain rates (SR)

Strain rate, the rate of deformation per second, calculates spatial differences in tissue velocities between adjacent myocardial regions and represents the regional contractility (Neil, 2002; Abraham et al, 2002). The quality of regional strain rate is highly dependent on both the insonation methodology and the acquisition frame rate. The atrial strain rate curve was characterized by the three main waves SR_S , SR_E , SR_A , which coincided with the ventricular systolic, early diastolic and late diastolic periods, respectively (Fig. 11b). In our studies, SR profile in the controls is distributed in a homogeneous pattern in the LA and RA walls respectively but the interatrial septal SR revealed inhomogeneous distribution with higher SR values in the mid segment than in the annular segment (Fig. 20), whereas velocities decreased from the annulus to mid segment and the strain rate showed the reversal pattern of distribution to that of the velocity in the interatrial septum. The superior segment mentioned above is less contractile and contributes no deformation in controls or patients with HCM. In patients with HCM the strain rate pattern had lost its inhomogeneity in IAS, but had similar homogenous distribution to healthy subjects in LA and RA walls respectively (Table 9 and Fig. 21).

4.14 Regional atrial performance in patients with HCM quantified by TD imaging

A pattern of impaired relaxation was previously evidenced in HCM patients by M-mode tissue Doppler imaging [141]. Our finding shows for the first time that regional atrial function is inhomogeneously impaired in patients with HCM. The reduced strain rate SR_S and SR_E peaks may reflect the decreased left ventricular function and increased atrial stiffness since the left atrium has no active motion in the ventricular systolic and early diastolic periods. The atrial contraction (SR_A) at the LA, IAS and RA is reduced which indicates a reduction of regional atrial pumping function in patients with HCM when compared with controls. The delayed ventricular relaxation in patients with HCM represented by prolongation of the septal IVRT is inversely correlated to the deformation in the left atrial wall. In contrast, IVRT is positively associated with the systolic right atrial deformation (SR_S), which may be a compensatory action due to the reduction of the left atrial regional function in HCM or due to atrial interaction. Reduced regional atrial function is not associated with the degree of IVS thickness in HCM patients, but the pressure load of the LV represented by the pressure gradient across the LVOT was negatively correlated to the regional atrial SR and early velocity. This means that an increase in the LV pressure load leads to more impairment of the LA regional function. Our data revealed for the first time new findings on the restricted atrial function, mainly in the LA, as a consequence of LV diastolic impairment due to hypertrophic changes involving the interventricular septum leading to pressure load on the LV in patients with HCM. Whether these findings were due to hemodynamic-dependent changes or to pathophysiological processes of HCM involving the atrial walls needs further comprehensive clinical study.

5 Summary and conclusions

Background

Hypertrophic cardiomyopathy (HCM) is a genetic disease, with autosomal dominant inheritance and a large number of mutations, characterized by cardiac hypertrophy, which is usually asymmetric and involves the interventricular septum, relaxation impairment, and global and regional dysfunction. HCM is the most frequent genetic cardiac muscle disease and the most common cause of sudden death in the young. Despite important medical advances in the past several years, assessment of myocardial function in HCM patients remains a diagnostic and therapeutic challenge for the cardiologist. Standard echocardiography is a simple method to diagnose hypertrophic cardiomyopathy. However, most of the currently available conventional echocardiographic techniques are semi-quantitative and are limited for a precise quantification of ventricular segmental contractile function, particularly, in those patients with obstructive forms of the HCM, atrial fibrillation or other arrhythmia, mitral regurgitation and SAM phenomenon. The new tissue Doppler imaging (TDI) potentially allows improved visual assessment of regional wall motion, provides quantitative information on several myocardial regions, and allows the measurement of myocardial velocities throughout the cardiac cycle, and the time intervals with high precision. More recently, the TDI-derived real-time strain rate (SRI) and strain technique has added further details to the above items by overcoming some of the limitations of the velocity measurements. Prior studies have validated the accuracy and reproducibility of velocity measures by TDI with in vitro models and in humans. Ventricular regional function and the effect of cardiac hypertrophy on atrial function by TDE have rarely been studied in patients with HCM.

Hypothesis: altered global and regional myocardial function in patients with HCM.

Aims

Quantitative assessment of the myocardial function in patients with HCM and to determine regional atrial function by non-invasive TDI, and strain/strain rate imaging.

Patients and methods

In the Deutsches Herzzentrum Berlin, 20 patients with HCM have been compared (regarding clinical and standard echocardiographic findings, tissue Doppler imaging and strain rate/strain imaging) to 20 age-matched normal subjects. Both groups were in NYHA class I-II. All patients and control group were examined with conventional echocardiography: parasternal long axis and

4 chamber view, M-mode, Doppler measurement of the flow at LVOT, RVOT, mitral and tricuspid valve and estimation of velocity and pressure gradient was done. TDI-derived velocity (S, E, A), strain rate (SR_S, SR_E, SR_A) and strain at the region of interest of LV, IVS, RV, LA, IAS, and RA were obtained. The related time intervals IVRT, IVCT, ET, FT and (Tei and I/H) indices were calculated.

Results

The study demonstrated the impairment of global and regional longitudinal systolic function in HCM patients as compared with normal subjects although the global function assessed by standard echocardiography was normal. In the patients with HCM the longitudinal regional systolic velocities are reduced and time required by the systolic velocity to reach its maximum is delayed. The reduction in the longitudinal velocities is more marked in the hypertrophied ventricular septum than in the lateral walls. Similarly, the systolic regional strain and strain rate (deformation) are reduced mainly in the IVS in patients with HCM. Strain is relative load-independent, whereas there was no correlation between strain and LVOT pressure gradient loading. The myocardial performance (Tei and I/H indices as parameters for global ventricular function) are significantly increased in patients with HCM when compared to controls. The left ventricular regional strain correlated to the global parameters, Tei index and I/H index, indicating a close relationship between the altered global and regional ventricular function in patients with HCM. The regional ventricular diastolic function is reduced in HCM patients; quantitative reduction of early, late diastolic velocity, E/A ratio, strain rate SR_E, and SR_A in the LV, IVS and RV walls.

RV global and regional systolic and diastolic function is impaired in patients with HCM as compared with the control group. However, despite the systolic impairment of regional RV function, a paradoxical increment of the regional SR_A at the basal segment was observed, which may be a compensatory action due to reduction of LV regional function. The clinical significance of this finding is unclear at this time, and further comprehensive study of the RV in patients with HCM is recommended. Qualitatively, in hypertrophied IVS deformation of the right side of the septum is faster than that of the left side, and strain is higher than that in the left side. This is due to the different architecture of the cardiac fibres within the left and right ventricle.

Regional atrial function, mainly regional diastolic left atrial function estimated by strain rate imaging in patients with HCM is restricted, probably due to the abnormal relaxation of the left

ventricle, leading to prolonged IVRT and impaired LV diastolic function and global myocardial performance or involvement of the atrial wall in the myopathic process.

Further comparative study of the atrial function with strain rate imaging in HCM patients with standard methodology like MRT is warranted, to validate the SRI as a useful tool measuring regional atrial function in HCM patients.

Conclusions

Tissue Doppler echocardiography is a non-invasive new technique; it is simple, reproducible and valuable in the assessment of regional and global cardiac function in patients with HCM. We demonstrate using strain/strain rate imaging and TD-derived parameters that the global and the regional systolic and diastolic function of LV and RV is impaired despite normal systolic function detected by conventional echocardiography in HCM patients. And for the first time the regional involvement of the atria mainly the left atrium and reduction of the regional atrial function in patients with HCM.

6 Zusammenfassung

Hintergrund

Die obstruktive hypertrophe Kardiomyopathie (HOCM) ist eine genetische Erkrankung, mit autosomal dominanter Vererbung und zahlreichen Mutationen. Sie ist durch eine asymmetrische Hypertrophie des interventrikulären Septums, Relaxationsstörung und Beeinträchtigung der globalen und regionalen myokardialen Funktion charakterisiert. Die HOCM ist die häufigste Ursache des plötzlichen Todes bei jungen Athleten. Trotz des Fortschrittes auf dem Gebiet der kardialen Diagnostik in den letzten Jahren, bleibt die Beurteilung der kardialen Funktion bei Kindern und Erwachsenen mit HCM eine diagnostische und therapeutische Herausforderung. Die Möglichkeiten der konventionellen Echokardiographie quantitative Informationen über die regionale myokardiale kontraktile Funktion zu liefern sind limitiert. Im Gegensatz dazu bietet die neue Gewebedoppler Echokardiographie die Möglichkeit genauere quantitative Information über die regionale systolische und diastolische Verlängerung und Verkürzung zu liefern. Die regionale ventrikuläre Funktion und der Einfluss der myokardialen Hypertrophie mit gestörter Relaxation auf die atriale Funktion mittels Gewebedoppler Echokardiographie ist bis jetzt nicht untersucht.

Hypothese: gestörte globale und regionale myokardiale Funktion bei Patienten mit HCM.

Ziele

Das Ziel dieser Arbeit war die Untersuchung der globalen und regionalen Kammerfunktion bei Patienten mit obstruktiver hypertropher Kardiomyopathie mittels der neuen Gewebedoppler Echokardiographie und anderen herkömmlichen Parametern. Die systolischen und diastolischen Myokardwandgeschwindigkeiten sowie ihre abgeleiteten Zeitintervalle, während eines Herzzyklus, sowie die isovolumetrische Kontraktion- und Relaxationszeit und daraus errechneten Indizien wurden bestimmt. Zusätzlich zur Analyse der Ventrikelfunktion wurde die Vorhoffunktion mittels der neuen Gewebedoppler Echokardiographie untersucht.

Patienten und Methoden

Zwanzig Patienten mit einem mittleren Alter von 18.6 (8.8) Jahre mit HOCM und 20 gleichaltrige gesunde Kontrollpersonen, wurden untersucht. 2-D Echokardiographie und Gewebedoppler Echokardiographie wurden bei allen Patienten und der Kontrollgruppe durchgeführt. In der parasternalen Längsachse wurde das M-Mode des linken Ventrikels gemessen. Die Einfluß- und Ausflußparameter des linken Ventrikels wurden im apikalen 4

Kammerblick bestimmt. Die Akquisition der Aufnahmen im Gewebedoppler-Modus wurden im apikalen 4 Kammerblick durchgeführt. Hier wurde drauf geachtet das die laterale Wand des LV, das intraventrikuläre Septum und die vordere freie RV-Wand mit den dazugehörigen atrialen Wänden separat mit dem geringsten Dopplerwinkel akquiriert werden sollten. Mit Hilfe einer speziellen Software (TVI; Vingmed Echopack, Horten, Norway) wurden dann die Myokardwandgeschwindigkeiten, der Strain und Strainwerte errechnet und analysiert.

Ergebnisse

Im Gegensatz zu den herkömmlichen Echoparametern zeigten die Gewebedoppler Parameter überwiegend eine abnorme regionale und globale Funktion bei Patienten mit HOCM im Vergleich zu der Kontrollgruppe an. Bei den Patienten mit HOCM sind die Gewebedoppler abgeleiteten Wandgeschwindigkeiten und ihre Zeitintervalle im Vergleich mit der Kontrollgruppe signifikant reduziert. Die Deformationsparameter des Myokards wie Strain und Strain rate sind bei den Patienten mit HOCM insbesondere im IVS signifikant reduziert. Andere aus den Einfluß- und Ausflußparametern abgeleitete Indizien für die globale Funktion wie der Tei- und I/H Index waren bei den Patienten mit HOCM ebenfalls abnorm verändert. Die regionale Myokarddeformation im LV korrelierte mit den Parametern der globalen Funktion bei den HOCM Patienten, jedoch nicht bei der Kontrollgruppe. Zusätzlich zu der Störung der globalen und regionalen Funktion des LV war die systolische Funktion des RV bei den Patienten mit HOCM abnorm verändert. Begleitend zu der abnorm reduzierten regionalen LV Funktion bei den HOCM Patienten wurde eine Erhöhung der ventrikulären Deformationsrate (Strain rate SR_A) im rechten Ventrikel beobachtet. Dies könnte auf eine kompensatorische Aktion des Ventrikel abnormer Relaxation hinweisen. Die klinische Bedeutung dieser Befunde bedarf jedoch weiterer Abklärung und Evaluation mit Hilfe anderer etablierter Methoden wie der MRT.

Schlussfolgerung

Die regionale und globale systolische und diastolische Funktion sind bei Patienten mit HOCM mit Hilfe der Gewebedoppler Echokardiographie evaluierbar und scheinen bei Patienten mit HOCM im Gegensatz zu der normalen Ejektionfraktion abnorm verändert zu sein. Strain und Strain rate sind möglicherweise vielversprechende nützliche Methoden zur Evaluation und Überwachung der regionalen Myokardfunktion im Vorhof und Ventrikel bei Patienten mit HOCM.

7 References

1. Wigle, E.D., et al., Hypertrophic cardiomyopathy. The importance of the site and the extent of hypertrophy. A review. *Prog Cardiovasc Dis*, 1985. 28(1): p. 1-83.
2. Karam, R., H.M. Lever, and B.P. Healy, Hypertensive hypertrophic cardiomyopathy or hypertrophic cardiomyopathy with hypertension? A study of 78 patients. *J Am Coll Cardiol*, 1989. 13(3): p. 580-4.
3. Maron, B.J., et al., Sudden death in young competitive athletes. Clinical, demographic, and pathological profiles. *Jama*, 1996. 276(3): p. 199-204.
4. Marian, A.J., L. Salek, and S. Lutucuta, Molecular genetics and pathogenesis of hypertrophic cardiomyopathy. *Minerva Med*, 2001. 92(6): p. 435-51.
5. Marian, A.J. and R. Roberts, The molecular genetic basis for hypertrophic cardiomyopathy. *J Mol Cell Cardiol*, 2001. 33(4): p. 655-70.
6. Niimura, H., et al., Mutations in the gene for cardiac myosin-binding protein C and late-onset familial hypertrophic cardiomyopathy. *N Engl J Med*, 1998. 338(18): p. 1248-57.
7. Maron, B.J., Hypertrophic cardiomyopathy: a systematic review. *Jama*, 2002. 287(10): p. 1308-20.
8. Maron, B.J., et al., American College of Cardiology/European Society of Cardiology clinical expert consensus document on hypertrophic cardiomyopathy. A report of the American College of Cardiology Foundation Task Force on Clinical Expert Consensus Documents and the European Society of Cardiology Committee for Practice Guidelines. *J Am Coll Cardiol*, 2003. 42(9): p. 1687-713.
9. Nishimura, R.A. and D.R. Holmes, Jr., Clinical practice. Hypertrophic obstructive cardiomyopathy. *N Engl J Med*, 2004. 350(13): p. 1320-7.
10. Subash Chandra, V., M. Jayranganth, and A.R. Shenoy, Non-surgical septal reduction for hypertrophic cardiomyopathy in childhood. *Int J Cardiol*, 2006. 106(3): p. 355-9.
11. Sanderson, J.E., et al., Left ventricular filling in hypertrophic cardiomyopathy. An angiographic study. *Br Heart J*, 1977. 39(6): p. 661-70.
12. Isaaz, K., et al., A new Doppler method of assessing left ventricular ejection force in chronic congestive heart failure. *Am J Cardiol*, 1989. 64(1): p. 81-7.
13. Heimdal, A., et al., Real-time strain rate imaging of the left ventricle by ultrasound. *J Am Soc Echocardiogr*, 1998. 11(11): p. 1013-9.
14. Urheim, S., et al., Myocardial strain by Doppler echocardiography. Validation of a new method to quantify regional myocardial function. *Circulation*, 2000. 102(10): p. 1158-64.

15. Kowalski, M., et al., Can natural strain and strain rate quantify regional myocardial deformation? A study in healthy subjects. *Ultrasound Med Biol*, 2001. 27(8): p. 1087-97.
16. Stoylen, A., et al., Strain rate imaging in normal and reduced diastolic function: comparison with pulsed Doppler tissue imaging of the mitral annulus. *J Am Soc Echocardiogr*, 2001. 14(4): p. 264-74.
17. Voigt, J.U., et al., Assessment of regional longitudinal myocardial strain rate derived from doppler myocardial imaging indexes in normal and infarcted myocardium. *J Am Soc Echocardiogr*, 2000. 13(6): p. 588-98.
18. Armstrong, G., et al., Use of peak systolic strain as an index of regional left ventricular function: comparison with tissue Doppler velocity during dobutamine stress and myocardial ischemia. *J Am Soc Echocardiogr*, 2000. 13(8): p. 731-7.
19. Edvardsen, T., et al., Regional myocardial systolic function during acute myocardial ischemia assessed by strain Doppler echocardiography. *J Am Coll Cardiol*, 2001. 37(3): p. 726-30.
20. Donovan, C.L., W.F. Armstrong, and D.S. Bach, Quantitative Doppler tissue imaging of the left ventricular myocardium: validation in normal subjects. *Am Heart J*, 1995. 130(1): p. 100-4.
21. Nikitin, N.P. and J.G. Cleland, [Use of myocardial tissue Doppler imaging in cardiology]. *Kardiologiia*, 2002. 42(3): p. 66-79.
22. Watari, T., et al., The usefulness of Doppler echocardiography for the evaluation of hemodynamics in tetralogy of Fallot: comparison of the patients with pre- and post-corrective surgery and control healthy children. *Acta Paediatr Jpn*, 1988. 30(5): p. 569-87.
23. Tei, C., New non-invasive index for combined systolic and diastolic ventricular function. *J Cardiol*, 1995. 26(2): p. 135-6.
24. Tei, C., et al., New index of combined systolic and diastolic myocardial performance: a simple and reproducible measure of cardiac function--a study in normals and dilated cardiomyopathy. *J Cardiol*, 1995. 26(6): p. 357-66.
25. Tei, C., et al., Noninvasive Doppler-derived myocardial performance index: correlation with simultaneous measurements of cardiac catheterization measurements. *J Am Soc Echocardiogr*, 1997. 10(2): p. 169-78.
26. Cassidy, D.M., et al., Endocardial mapping in humans in sinus rhythm with normal left ventricles: activation patterns and characteristics of electrograms. *Circulation*, 1984. 70(1): p. 37-42.

27. Lundback, S., Cardiac pumping and function of the ventricular septum. *Acta physiol Scand suppl*, 1986. 550: p. 101.
28. Schminke, A., Ueber linkseitige muskuelare Conusstenosen. *Deutsch Med Wochenschr*, 1907. 22: p. 2083.
29. Jamal, F., et al., Quantification of the spectrum of changes in regional myocardial function during acute ischemia in closed chest pigs: an ultrasonic strain rate and strain study. *J Am Soc Echocardiogr*, 2001. 14(9): p. 874-84.
30. Jamal, F., et al., Longitudinal strain quantitates regional right ventricular contractile function. *Am J Physiol Heart Circ Physiol*, 2003. 285(6): p. H2842-7.
31. Weidemann, F., B. Eyskens, and G.R. Sutherland, New ultrasound methods to quantify regional myocardial function in children with heart disease. *Pediatr Cardiol*, 2002. 23(3): p. 292-306.
32. Tekten, T., et al., Novel approach to measure myocardial performance index: pulsed-wave tissue Doppler echocardiography. *Echocardiography*, 2003. 20(6): p. 503-10.
33. Schaefer, A., et al., Evaluation of Tissue Doppler Tei index for global left ventricular function in mice after myocardial infarction: comparison with Pulsed Doppler Tei index. *Eur J Echocardiogr*, 2005. 6(5): p. 367-75.
34. Thomas, L., et al., Changes in regional left atrial function with aging: evaluation by Doppler tissue imaging. *Eur J Echocardiogr*, 2003. 4(2): p. 92-100.
35. Vulpian, M., retrecissement mitral. concretion sanguine. retrecissement sous-aortique du ventricle gauche. *Bull Soc Anat Paris* 1868. 43: p. 2078.
36. Brock, R., Functional obstruction of the left ventricle; acquired aortic subvalvar stenosis. *Guys Hosp Rep*, 1957. 106(4): p. 221-38.
37. Nagueh, S.F., et al., Comparison of ethanol septal reduction therapy with surgical myectomy for the treatment of hypertrophic obstructive cardiomyopathy. *J Am Coll Cardiol*, 2001. 38(6): p. 1701-6.
38. Maron, B.J., et al., Prevalence of hypertrophic cardiomyopathy in a general population of young adults. Echocardiographic analysis of 4111 subjects in the CARDIA Study. Coronary Artery Risk Development in (Young) Adults. *Circulation*, 1995. 92(4): p. 785-9.
39. McKenna, W., et al., Prognosis in hypertrophic cardiomyopathy: role of age and clinical, electrocardiographic and hemodynamic features. *Am J Cardiol*, 1981. 47(3): p. 532-8.
40. Schulte, H.D., et al., Management of symptomatic hypertrophic obstructive cardiomyopathy--long-term results after surgical therapy. *Thorac Cardiovasc Surg*, 1999. 47(4): p. 213-8.

41. Elliott, P.M., et al., Sudden death in hypertrophic cardiomyopathy: identification of high risk patients. *J Am Coll Cardiol*, 2000. 36(7): p. 2212-8.
42. Maron, B.J., et al., Efficacy of implantable cardioverter-defibrillators for the prevention of sudden death in patients with hypertrophic cardiomyopathy. *N Engl J Med*, 2000. 342(6): p. 365-73.
43. Vosberg, H.P., Genetic counselling for hypertrophic cardiomyopathy: are we ready for it? *Curr Control Trials Cardiovasc med*, 2000. 1(1): p. 41-44.
44. Prasad, K. and M.P. Frenneaux, Sudden death in hypertrophic cardiomyopathy: potential importance of altered autonomic control of vasculature. *Heart*, 1998. 79(6): p. 538-40.
45. Yetman, A.T. and B.W. McCrindle, Management of pediatric hypertrophic cardiomyopathy. *Curr Opin Cardiol*, 2005. 20(2): p. 80-3.
46. Konno, T., et al., A novel mutation in the cardiac myosin-binding protein C gene is responsible for hypertrophic cardiomyopathy with severe ventricular hypertrophy and sudden death. *Clin Sci (Lond)*, 2006. 110(1): p. 125-31.
47. Ko, Y.L., et al., Genetic heterogeneity for familial hypertrophic cardiomyopathy in Chinese: analysis of six Chinese kindreds. *Chin Med J (Engl)*, 1998. 111(5): p. 416-21.
48. Alizad, A. and J.B. Seward, Echocardiographic features of genetic diseases: part 1. Cardiomyopathy. *J Am Soc Echocardiogr*, 2000. 13(1): p. 73-86.
49. Roberts, R. and U. Sigwart, New concepts in hypertrophic cardiomyopathies, part I. *Circulation*, 2001. 104(17): p. 2113-6.
50. Roberts, R. and U. Sigwart, New concepts in hypertrophic cardiomyopathies, part II. *Circulation*, 2001. 104(18): p. 2249-52.
51. Chung, M.W., T. Tsoutsman, and C. Semsarian, Hypertrophic cardiomyopathy: from gene defect to clinical disease. *Cell Res*, 2003. 13(1): p. 9-20.
52. Woo, A., et al., Mutations of the beta myosin heavy chain gene in hypertrophic cardiomyopathy: critical functional sites determine prognosis. *Heart*, 2003. 89(10): p. 1179-85.
53. Lev, D., et al., Clinical presentations of mitochondrial cardiomyopathies. *Pediatr Cardiol*, 2004. 25(5): p. 443-50.
54. Elliott, P. and W.J. McKenna, Hypertrophic cardiomyopathy. *Lancet*, 2004. 363(9424): p. 1881-91.
55. Maron, B.J., et al., Impact of laboratory molecular diagnosis on contemporary diagnostic criteria for genetically transmitted cardiovascular diseases: hypertrophic cardiomyopathy, long-QT syndrome, and Marfan syndrome. A statement for healthcare professionals from

- the Councils on Clinical Cardiology, Cardiovascular Disease in the Young, and Basic Science, American Heart Association]. *Circulation*, 1998. 98(14): p. 1460-71.
56. Rosenzweig, A., et al., Preclinical diagnosis of familial hypertrophic cardiomyopathy by genetic analysis of blood lymphocytes. *N Engl J Med*, 1991. 325(25): p. 1753-60.
 57. Wigle, E.D., et al., Hypertrophic cardiomyopathy. Clinical spectrum and treatment. *Circulation*, 1995. 92(7): p. 1680-92.
 58. Wigle, E.D., *Cardiomyopathy: The diagnosis of hypertrophic cardiomyopathy*. *Heart*, 2001. 86(6): p. 709-14.
 59. Miroslawa, U., Hypertrophic cardiomyopathy: history and novel insights into pathogenesis and pathologic mechanism. *Mon sci monit*, 1997. 3(4): p. 618.
 60. Spirito, P. and B.J. Maron, Absence of progression of left ventricular hypertrophy in adult patients with hypertrophic cardiomyopathy. *J Am Coll Cardiol*, 1987. 9(5): p. 1013-7.
 61. Prasad, K., et al., Echocardiographic pitfalls in the diagnosis of hypertrophic cardiomyopathy. *Heart*, 1999. 82 Suppl 3: p. III8-III15.
 62. Eidem, B.W., C. Jones, and F. Cetta, Unusual association of hypertrophic cardiomyopathy with complete atrioventricular canal defect and Down syndrome. *Tex Heart Inst J*, 2000. 27(3): p. 289-91.
 63. Bryant, R.M., Hypertrophic cardiomyopathy in children. *Cardiol Rev*, 1999. 7(2): p. 92-100.
 64. Ostman-Smith, I., G. Wettrell, and T. Riesenfeld, A cohort study of childhood hypertrophic cardiomyopathy: improved survival following high-dose beta-adrenoceptor antagonist treatment. *J Am Coll Cardiol*, 1999. 34(6): p. 1813-22.
 65. Pacileo, G., et al., Hypertrophic cardiomyopathy in pediatric patients: effect of verapamil on regional and global left ventricular diastolic function. *Can J Cardiol*, 2000. 16(2): p. 146-52.
 66. Sherrid, M.V., et al., Multicenter study of the efficacy and safety of disopyramide in obstructive hypertrophic cardiomyopathy. *J Am Coll Cardiol*, 2005. 45(8): p. 1251-8.
 67. Maron, B.J., Sudden death in young athletes. *N Engl J Med*, 2003. 349(11): p. 1064-75.
 68. Ralph-Edwards, A., et al., Hypertrophic obstructive cardiomyopathy: comparison of outcomes after myectomy or alcohol ablation adjusted by propensity score. *J Thorac Cardiovasc Surg*, 2005. 129(2): p. 351-8.
 69. Firoozi, S., et al., Septal myotomy-myectomy and transcatheter septal alcohol ablation in hypertrophic obstructive cardiomyopathy. A comparison of clinical, haemodynamic and exercise outcomes. *Eur Heart J*, 2002. 23(20): p. 1617-24.

70. Minakata, K., et al., Mechanisms for recurrent left ventricular outflow tract obstruction after septal myectomy for obstructive hypertrophic cardiomyopathy. *Ann Thorac Surg*, 2005. 80(3): p. 851-6.
71. Thomas, B., Hypertrophic cardiomyopathy: therapeutic approaches. *Heart Dis*, 1999. 1(2): p. 91-7.
72. Sherrid, M.V., D. Gunsburg, and A. Sharma, Medical treatment of hypertrophic cardiomyopathy. *Curr Cardiol Rep*, 2000. 2(2): p. 148-53.
73. Golledge, P. and C.J. Knight, Current management of hypertrophic cardiomyopathy. *Hosp Med*, 2001. 62(2): p. 79-82.
74. Pellnitz, C., et al., [Sudden cardiac death in familial hypertrophic cardiomyopathy. Identification of high-risk patients]. *Dtsch Med Wochenschr*, 2005. 130(18): p. 1150-4.
75. Seggewiss, Management of hypertrophic cardiomyopathy in children. *Pediatric drugs*, 2003. 5(10): p. 10.
76. Wandt, B., Long-axis contraction of the ventricles: a modern approach, but described already by Leonardo da Vinci. *J Am Soc Echocardiogr*, 2000. 13(7): p. 699-706.
77. Cardim, N., et al., Tissue Doppler imaging in hypertrophic cardiomyopathy: impact of intraventricular obstruction on longitudinal left ventricular function. *Rev Port Cardiol*, 2002. 21(3): p. 271-97.
78. Miyatake, K., et al., New method for evaluating left ventricular wall motion by color-coded tissue Doppler imaging: in vitro and in vivo studies. *J Am Coll Cardiol*, 1995. 25(3): p. 717-24.
79. Yamazaki, N., Analysis of ventricular wall motion using colour-coded tissue Doppler imaging system *JPN J Appl Phys*, 1994. 33: p. 3146.
80. Palka, P., et al., Differences in myocardial velocity gradient measured throughout the cardiac cycle in patients with hypertrophic cardiomyopathy, athletes and patients with left ventricular hypertrophy due to hypertension. *J Am Coll Cardiol*, 1997. 30(3): p. 760-8.
81. Shimizu, Y., et al., Peak negative myocardial velocity gradient in early diastole as a noninvasive indicator of left ventricular diastolic function: comparison with transmitral flow velocity indices. *J Am Coll Cardiol*, 1998. 32(5): p. 1418-25.
82. Gulati, V.K., et al., Mitral annular descent velocity by tissue Doppler echocardiography as an index of global left ventricular function. *Am J Cardiol*, 1996. 77(11): p. 979-84.
83. Yamada, H., et al., Assessment of left ventricular systolic wall motion velocity with pulsed tissue Doppler imaging: comparison with peak dP/dt of the left ventricular pressure curve. *J Am Soc Echocardiogr*, 1998. 11(5): p. 442-9.

84. Galiuto, L., G. Ignone, and A.N. DeMaria, Contraction and relaxation velocities of the normal left ventricle using pulsed-wave tissue Doppler echocardiography. *Am J Cardiol*, 1998. 81(5): p. 609-14.
85. Kukulski, T., et al., Normal regional right ventricular function and its change with age: a Doppler myocardial imaging study. *J Am Soc Echocardiogr*, 2000. 13(3): p. 194-204.
86. Galderisi, M., et al., Myocardial diastolic impairment caused by left ventricular hypertrophy involves basal septum more than other walls: analysis by pulsed Doppler tissue imaging. *J Hypertens*, 1999. 17(5): p. 685-93.
87. Pela, G., et al., Doppler tissue echocardiography: myocardial wall motion velocities in essential hypertension. *Eur J Echocardiogr*, 2001. 2(2): p. 108-17.
88. Balci, B. and O. Yilmaz, Influence of left ventricular geometry on regional systolic and diastolic function in patients with essential hypertension. *Scand Cardiovasc J*, 2002. 36(5): p. 292-6.
89. Phadke, R.S., et al., Hypertrophic cardiomyopathy: an autopsy analysis of 14 cases. *J Postgrad Med*, 2001. 47(3): p. 165-70.
90. Ahmad, M., et al., An autopsy study of hypertrophic cardiomyopathy. *J Pak Med Assoc*, 2003. 53(10): p. 459-62.
91. Hughes, S.E., The pathology of hypertrophic cardiomyopathy. *Histopathology*, 2004. 44(5): p. 412-27.
92. Greenberg, N.L., et al., Doppler-derived myocardial systolic strain rate is a strong index of left ventricular contractility. *Circulation*, 2002. 105(1): p. 99-105.
93. Weidemann, F., et al., Quantification of regional left and right ventricular radial and longitudinal function in healthy children using ultrasound-based strain rate and strain imaging. *J Am Soc Echocardiogr*, 2002. 15(1): p. 20-8.
94. Naito, H., et al., Assessment of right ventricular regional contraction and comparison with the left ventricle in normal humans: a cine magnetic resonance study with presaturation myocardial tagging. *Br Heart J*, 1995. 74(2): p. 186-91.
95. Dagdeviren, B., et al., [Value of tissue Doppler imaging in the determination of the right ventricular systolic function]. *Anadolu Kardiyol Derg*, 2001. 1(2): p. 85-9, AXIII-AXIV.
96. Efthimiadis, G.K., et al., Doppler echocardiographic evaluation of right ventricular diastolic function in hypertrophic cardiomyopathy. *Eur J Echocardiogr*, 2002. 3(2): p. 143-8.
97. Eidem, B.W., et al., Usefulness of the myocardial performance index for assessing right ventricular function in congenital heart disease. *Am J Cardiol*, 2000. 86(6): p. 654-8.

98. Aoki, M., et al., Quantitative assessment of right ventricular function using doppler tissue imaging in fetuses with and without heart failure. *J Am Soc Echocardiogr*, 2004. 17(1): p. 28-35.
99. Yasuoka, K., et al., Tei index determined by tissue Doppler imaging in patients with pulmonary regurgitation after repair of tetralogy of Fallot. *Pediatr Cardiol*, 2004. 25(2): p. 131-6.
100. Mouloupoulos, S.D., et al., Left ventricular performance during by-pass or distension of the right ventricle. *Circ Res*, 1965. 17(6): p. 484-91.
101. Laks, M.M., D. Garner, and H.J. Swan, Volumes and compliances measured simultaneously in the right and left ventricles of the dog. *Circ Res*, 1967. 20(5): p. 565-9.
102. Taylor, R.R., et al., Dependence of ventricular distensibility on filling of the opposite ventricle. *Am J Physiol*, 1967. 213(3): p. 711-8.
103. Bemis, C.E., et al., Influence of right ventricular filling pressure on left ventricular pressure and dimension. *Circ Res*, 1974. 34(4): p. 498-504.
104. Elzinga, G., et al., Ventricular interference. *Am J Physiol*, 1974. 226(4): p. 941-7.
105. Santamore, W.P. and L.J. Dell'Italia, Ventricular interdependence: significant left ventricular contributions to right ventricular systolic function. *Prog Cardiovasc Dis*, 1998. 40(4): p. 289-308.
106. Santamore, W.P., et al., Left ventricular effects on right ventricular developed pressure. *J Appl Physiol*, 1976. 41(6): p. 925-30.
107. Santamore, W.P., et al., Myocardial interaction between the ventricles. *J Appl Physiol*, 1976. 41(3): p. 362-8.
108. Scharf, S.M., et al., Effects of normal and loaded spontaneous inspiration on cardiovascular function. *J Appl Physiol*, 1979. 47(3): p. 582-90.
109. Janicki, J.S. and K.T. Weber, The pericardium and ventricular interaction, distensibility, and function. *Am J Physiol*, 1980. 238(4): p. H494-503.
110. Weber, K.T., et al., Contractile mechanics and interaction of the right and left ventricles. *Am J Cardiol*, 1981. 47(3): p. 686-95.
111. Clyne, C.A., J.S. Alpert, and J.R. Benotti, Interdependence of the left and right ventricles in health and disease. *Am Heart J*, 1989. 117(6): p. 1366-73.
112. Oh, J.K., et al., Diagnostic role of Doppler echocardiography in constrictive pericarditis. *J Am Coll Cardiol*, 1994. 23(1): p. 154-62.

113. Hurrell, D.G., et al., Value of dynamic respiratory changes in left and right ventricular pressures for the diagnosis of constrictive pericarditis. *Circulation*, 1996. 93(11): p. 2007-13.
114. Yamaguchi, S., et al., Effect of left ventricular volume on right ventricular end-systolic pressure-volume relation. Resetting of regional preload in right ventricular free wall. *Circ Res*, 1989. 65(3): p. 623-31.
115. Slinker, B.K., A.C. Chagas, and S.A. Glantz, Chronic pressure overload hypertrophy decreases direct ventricular interaction. *Am J Physiol*, 1987. 253(2 Pt 2): p. H347-57.
116. Brown, C.D., E. Chow, and D.J. Farrar, Left ventricular unloading decreases rate of isovolumic right ventricular pressure decline. *Am J Physiol*, 1993. 265(5 Pt 2): p. H1663-9.
117. Oyama, S., et al., Right ventricular systolic function and the manner of transformation of the right ventricle in patients with dilated cardiomyopathy. *Circ J*, 2004. 68(10): p. 933-7.
118. Severino, S., et al., Involvement of right ventricle in left ventricular hypertrophic cardiomyopathy: analysis by pulsed Doppler tissue imaging. *Eur J Echocardiogr*, 2000. 1(4): p. 281-8.
119. Koyama, J., P.A. Ray-Sequin, and R.H. Falk, Longitudinal myocardial function assessed by tissue velocity, strain, and strain rate tissue Doppler echocardiography in patients with AL (primary) cardiac amyloidosis. *Circulation*, 2003. 107(19): p. 2446-52.
120. Slordahl, S.A., et al., High frame rate strain rate imaging of the interventricular septum in healthy subjects. *Eur J Ultrasound*, 2001. 14(2-3): p. 149-55.
121. Hoffmann, R., et al., Strain rate measurement by doppler echocardiography allows improved assessment of myocardial viability in patients with depressed left ventricular function. *J Am Coll Cardiol*, 2002. 39(3): p. 443-9.
122. Yang, H., et al., Use of strain imaging in detecting segmental dysfunction in patients with hypertrophic cardiomyopathy. *J Am Soc Echocardiogr*, 2003. 16(3): p. 233-9.
123. Eidem, B.W., et al., Nongeometric quantitative assessment of right and left ventricular function: myocardial performance index in normal children and patients with Ebstein anomaly. *J Am Soc Echocardiogr*, 1998. 11(9): p. 849-56.
124. Tei, C., et al., Doppler echocardiographic index for assessment of global right ventricular function. *J Am Soc Echocardiogr*, 1996. 9(6): p. 838-47.
125. Tei, C., et al., Doppler index combining systolic and diastolic myocardial performance: clinical value in cardiac amyloidosis. *J Am Coll Cardiol*, 1996. 28(3): p. 658-64.
126. LaCorte, J.C., et al., Correlation of the Tei index with invasive measurements of ventricular function in a porcine model. *J Am Soc Echocardiogr*, 2003. 16(5): p. 442-7.

127. Tsutsumi, T., et al., Serial evaluation for myocardial performance in fetuses and neonates using a new Doppler index. *Pediatr Int*, 1999. 41(6): p. 722-7.
128. Mori, Y., et al., Evaluation of systolic and diastolic ventricular performance of the right ventricle in fetuses with ductal constriction using the Doppler Tei index. *Am J Cardiol*, 2001. 88(10): p. 1173-8.
129. Williams, R.V., et al., Quantitative assessment of ventricular function in children with single ventricles using the Doppler myocardial performance index. *Am J Cardiol*, 2000. 86(10): p. 1106-10.
130. Ishii, M., et al., Quantitation of the global right ventricular function in children with normal heart and congenital heart disease: a right ventricular myocardial performance index. *Pediatr Cardiol*, 2000. 21(5): p. 416-21.
131. Yeo, T.C., et al., Value of a Doppler-derived index combining systolic and diastolic time intervals in predicting outcome in primary pulmonary hypertension. *Am J Cardiol*, 1998. 81(9): p. 1157-61.
132. Eto, G., et al., Assessment of global left ventricular function in normal children and in children with dilated cardiomyopathy. *J Am Soc Echocardiogr*, 1999. 12(12): p. 1058-64.
133. Kim, W.H., et al., Estimation of left ventricular function in right ventricular volume and pressure overload. Detection of early left ventricular dysfunction by Tei index. *Jpn Heart J*, 1999. 40(2): p. 145-54.
134. Sebbag, I., et al., Effect of chronic infusion of epoprostenol on echocardiographic right ventricular myocardial performance index and its relation to clinical outcome in patients with primary pulmonary hypertension. *Am J Cardiol*, 2001. 88(9): p. 1060-3.
135. Harada, K., et al., Comparison of the right ventricular Tei index by tissue Doppler imaging to that obtained by pulsed Doppler in children without heart disease. *Am J Cardiol*, 2002. 90(5): p. 566-9.
136. Tekten, T., et al., Value of measuring myocardial performance index by tissue Doppler echocardiography in normal and diseased heart. *Jpn Heart J*, 2003. 44(3): p. 403-16.
137. Toma, y., Left atrial filling in normal human subjects: relation between left atrial contraction and left atrial early filling. *Cardiovasc Res*, 1987. 214: p. 259.
138. Miyaguchi, K., et al., Role of left atrial booster pump function in a worsening course of congestive heart failure. *Jpn Circ J*, 1992. 56(5): p. 509-17.
139. Hoit, B.D. and R.A. Walsh, Regional atrial distensibility. *Am J Physiol*, 1992. 262(5 Pt 2): p. H1356-60.

140. Shively, B.K., E.A. Gelgand, and M.H. Crawford, Regional left atrial stasis during atrial fibrillation and flutter: determinants and relation to stroke. *J Am Coll Cardiol*, 1996. 27(7): p. 1722-9.
141. Cardim, N., et al., Regional diastolic function in hypertrophic cardiomyopathy: a tissue Doppler echocardiographic study. *Rev Port Cardiol*, 1997. 16(7-8): p. 615-9, 588.

8 Figure/Table index

8.1 Figures

Figure 1: Myocardial hypertrophy of both ventricles in one month old child with HCM (A, B)...	8
Figure 2: Calculation of cardiac cycles intervals.	13
Figure 3: The pattern of myocardial longitudinal velocity deformations, systolic (S), early diastolic (E) and late diastolic (A) waves of the mid segments of interventricular septum in controls (A) and HCM patients (B).....	15
Figure 4: Velocity integral (mm) at mid IVS-wall in controls (A) and patients with HCM (B) ..	16
Figure 5: Pattern of strain rate curve at the IVS wall in controls (A) and in HCM patients (B) ..	16
Figure 6: An example of myocardial strain pattern in normal subject.....	17
Figure 7: Pattern of normal strain in IVS of controls(A) and abnormal strain at IVS in HCM patients (B)	17
Figure 8: Tissue Doppler and cardiac cycle intervals.	18
Figure 9: Cardiac cycle intervals timing presented according to changes with basal septal velocity trace, colour curved M-mode tissue Doppler and anatomical M-mode velocity trace. ...	19
Figure 10: Sites of velocity samples at the annular and mid segments of the atrial walls.....	20
Figure 11: Pattern of atrial regional velocity (A) and strain rate at IAS annular segments in controls (B).....	21
Figure 12: Distribution of clinical manifestations in the paediatric patients studied.....	23
Figure 13: The distribution of patient ages at the time of initial manifestation of HCM.....	23
Figure 14: Abnormal cardiac and non-cardiac conditions associated with hypertrophic cardiomyopathy	23
Figure 15: Abnormal echocardiographic findings in patients with HCM.....	23
Figure 16: Comparison of ventricular regional strain rate values at different points of myocardial segments between HCM and controls	27
Figure 17: Significant delay of systolic (s) myocardial velocities to reach its peak in HCM patients at different myocardial segments in comparison to controls	28
Figure 18: The longitudinal ventricular velocity integral (displacement in cm) was significantly reduced in patients with HCM.	29
Figure 19: Difference in atrial velocities between annular and mid segments	33
Figure 20: Distribution of atrial segmental velocity in patients with HCM.....	34
Figure 21: Distribution of strain rate in atrial segments in controls.....	35
Figure 22: Distribution of strain rate in atrial wall segments in HCM.....	36

8.2 Tables

Table 1: Classification of hypertrophic cardiomyopathy.....	9
Table 2: Main applications of tissue Doppler imaging in cardiology.....	11
Table 3: Patients' characteristics (n = 20).....	22
Table 4: Echocardiographic findings Echocardiographic findings of 20 patients with HCM in comparison to 20 controls.	25
Table 5: Comparison between the longitudinal ventricular segmental velocities (cm/s) in HCM patients (n=20) and controls (n=20), (mean \pm SD)	26
Table 6: Comparison between the strain in HCM and controls at different segments.....	30
Table 7: Tissue Doppler parameters in interventricular septum of HCM and control patients	31
Table 8: Comparison between the segmental delayed atrial velocity (cm/s) in HCM (n=20) and controls (n=20), (mean \pm SD)	33
Table 9: Comparison between the atrial strain rate (1/S) in HCM (n = 20) and controls (n = 20) (mean \pm SD)	34
Table 10: Comparison of time intervals and indices between HCM to controls	37
Table 11: The WHO classification of cardiomyopathy:	38
Table 12: The Factors that increase the risk of sudden death in patients with hypertrophic cardiomyopathy	39

9 Acknowledgement

I am greatly honored to express my profound gratitude and cordial appreciation to Priv.-Doz. Dr. med. Hashim Abdul Khaliq for adoption of this thesis, help in planning and preparing the present study and for his kindness, enthusiasm, persistent encouragement and sincere help.

I am also greatly obliged and indebted to Prof. Dr. med. P.E. Lange the former Director of the Clinic for congenital heart disease and the new Director Prof. Dr. med. F. Berger for their generous assistance, continuous guidance.

Finally, I would like to take this occasion to send my warmest thanks to the “General Secretary of High Education and General Secretary of Health in Libya” for their financial and moral support without it this work could never be finished.

10 Statement

Here I am stating that I submit the “Medizinische Fakultät der Charité-Universitätsmedizin Berlin” my MD theseis titled “**Evaluation of the myocardial function in patients with hypertrophic obstructive cardiomyopathy by tissue Doppler technique**” aming for academic (MD) promotion.

This work originates from“ Deutsches Herzzentrum Berlin” with the support from PD Dr. H. Abdul-Khaliq, Prof. Dr. med. P.E. Lange and Prof. Dr. med. F. Berger was performed with out any other help. With the completion of this work the right of a third person was not injured.

Till now this work was not send to any indoors or outdoors faculties. The “Medizinische Fakultät der Charité-Universitätsmedizin Berlin” has the right to do further copies of this work.

Berlin 07.07.2007

Ragiab Telagh

11 Curriculum Vitae

“Mein Lebenslauf wird aus Datenschutzgründen in der elektronischen Version meiner Arbeit nicht mit veröffentlicht“

Publications

1. Telagh RA, Schlüter B, Buschatz D et al. : Das obstruktive Schlaf-Apnoe-Syndrom (OSAS) im Kindesalter: Klinische und polysomnographische Befunde vor und nach Adenotomie und Tonsillektomie. *Somnologie* 1999; 3: 270-276.
2. Telagh R, Abdul-Khaliq H, Nürnberg JH, Alexi-Meskishvili V, Hetzer R, Berger F, Lange PE. Hypertrophe obstruktive Kardiomyopathie (HOCM) im Kindesalter: initiale Symptomatik und Therapie. In: Abstraktband der 50. Jahrestagung der Norddeutschen Gesellschaft für Kinderheilkunde und Jugendmedizin. Hamburg : Omnimed, 2001: 59.
3. Telagh R, Abdul-Khaliq H, Schubert S, Alexi-Meskishvili V, Hübler M, Lange PE. Double chambered right ventricle. Klinische Präsentation und chirurgische Behandlung bei 16 Patienten. 34. Jahrestagung der Deutschen Gesellschaft für Pädiatrische Kardiologie, Bamberg, 5-8.10.2002. *Z Kardiol* 2002; 91(9):757.
4. Telagh R, Abd El Rahman MY, Hui W, Lange PE, Berger F, Abdul-Khaliq H. Quantitative assessment of regional and global longitudinal ventricular dysfunction in patients with hypertrophic cardiomyopathies (HCM) using tissue Doppler imaging (TDI). 40th Annual General Meeting of the Association for European Paediatric Cardiology, Copenhagen, 18-21.5.2005. *Cardiol Young* 2005;15(Suppl 2): 53-54.
5. Telagh R, Abd El Rahman MY, Hui W, Lange PE, Berger F, Abdul-Khaliq H. Evaluation of atrial function in patients with hypertrophic cardiomyopathies (HCM) using tissue Doppler imaging (TDI). 41th Annual General Meeting of the Association for European Paediatric Cardiology, Basel, May 24 -27, 2006.

Berlin 07.07.2007